J Solid State Electrochem (2009) 13:3–25
DOI 10.1007/s10008-008-0556-9

REVIEW

Solid-state potentiometric gas sensors—current status and future trends

P. Pasierb · M. Rekas

Received: 5 March 2008 / Accepted: 1 April 2008 / Published online: 6 May 2008

Abstract The development of potentiometric sensors for monitoring environmental gases has become a well-established direction in sensor technology. Various types of potentiometric sensors employing solid electrolytes for in situ measurements of such gases as oxygen, hydrogen, carbon dioxide, sulfur oxides, carbon monoxide, nitrogen oxides, and hydrocarbons are reviewed. Particular concern was given to the CO_2 potentiometric sensor which is an example of successful commercial application. The construction details, working mechanism, and performance of different types of potentiometric gas sensors are given. Special emphasis is given for the mixed-potential electrodes, which seems to be the principal direction for the future research and development of the sensor science and technology. Additionally, the future use of potentiometric sensors for the detection of other environmental gases is discussed.

Keywords Potentiometric gas sensors · Solid electrolytes

Introduction

There is significant activity in the development of new sensor technology for monitoring of environmental gases. Several concepts for gas sensors are now under consideration. Chemical gas sensors may be classified into three main categories. The first group is composed of sensors generally based on the generation of voltage and currents in potentiometric cells using liquid or solid electrolytes. The second category includes sensors based on materials which change their physical properties, such as surface electrical conductivity, gate effects in the characteristics of field-effect transistors and metal–oxide–silicon (MOS) structures, Curie points for piezoelectric and Hall-effect devices, and adsorption bands for optical devices [1, 2]. The third type of sensors includes catalytic combustion gas sensors operating as submicro-calorimeters.

The need for reliable, sensitive, and stable sensors is caused by a growing trend to lower the levels of concentration at which potential pollutants have to be monitored and controlled, according to what is required in many industrial applications. With the increase in environmental deterioration caused by acid precipitation, on-site measurement of acid-forming gases is desirable. Large coal-fired and oil-fired facilities are under heavy pressure to reduce the emissions of sulfur oxides (SO_x), nitrogen oxides (NO_x) and carbon oxides (CO_x) [3, 4].

Sulfur is one of the main organic impurities in fossil fuels [5]. Nitrogen oxides (NO and NO_2) are products of direct synthesis occurring at high temperatures. They are mainly emitted from automobiles, stationary combustion facilities, and homes. The interest in sulfur recovery and in the monitoring of SO_x and NO_x emissions continues to remain high because ‘it is market-driven in stringent government regulations, especially the enactment of the Clean Air Act Amendments (CAAA) of 1990 with additional US State regulations for reducing SO_x and NO_x in coal-fired boiler emissions by 90% and above’ [6, 7]. Many years of financial and intellectual effort have gone into identifying possible practical solutions. The 1990s revolution relating to the development of the in situ SO_x and NO_x combustion gas analyzers continues unabated as new analyzers are combined with microprocessor technology to produce more powerful capabilities.

Carbon dioxide concentration in air has risen from a pre-industrial level of about 265 ppm [8] to a value above

P. Pasierb (✉) · M. Rekas
Faculty of Materials Science and Ceramics,
AGH University of Science and Technology,
al. Mickiewicza 30,
30-059 Krakow, Poland
e-mail: ppasierb@agh.edu.pl

355 ppm (1995), and recent reports [9, 10] suggest that by 2050, this value will have increased to 710 ppm. This steady CO_2 increase contributes to global warming. The most effective way of suppressing CO_2 exhaustion into the atmosphere is to control the emission amount of CO_2 at every exhaust site. For this purpose, simple inexpensive and portable sensors need to be developed.

Since the incomplete combustion of fuel sometimes causes serious carbon monoxide (CO) and hydrocarbon (CH_x) poisoning, the sensing of toxic, odorless CO has recently become increasingly important with regard to the safety of gas appliances. As a consequence of this, compact solid-state CO and CH_x sensors are needed in order to detect the incomplete combustion of gas appliances. For the above uses, the sensors should have high CO sensitivity combined with high CO selectivity against coexistent CO_2, NO_x, H_2, H_2O, and hydrocarbon gases. The development of CH_x and CO sensors is particularly important in the prevention of unexpected explosions and fires in mines [11].

Although a variety of sensor development efforts may be found in the literature now, it is important to note that most of these developments are based on empirical methods, mainly trial and error [11]. Unfortunately, most of the investigated prototype sensors are not always directly applicable for making reliable measurements in the harsh industrial environments found in the steel, heat treating, metal casting, glass, ceramic, pulp and paper, automotive, utility, and power industries, agriculture, and coal mines. Moreover, a fundamental understanding of the sensing mechanism is missing, and this makes the optimization of the sensor's design a very important task.

The objective of this paper is to review the developing field of potentiometric sensors for the detection and measurement of important environmental gases such as hydrogen, oxygen, carbon dioxide, sulfur and nitrogen oxides, and other gases.

Until now, a number of papers describing electrochemical devices as sensors for various gases have been published. Depending on the type of measured signal, electrochemical sensors may be divided into three general groups: potentiometric, amperometric, and coulometric. Additionally, taking into account the structure details of the gas sensors, the other classification has been proposed by Weppner [2, 12] and then further developed by Yamazoe and Miura [13].

Conventional solid-state ionic sensors (type I)

In the case of conventional potentiometric gas sensors, the gas to be detected is converted to the mobile component in a solid electrolyte (Fig. 1). The solid electrolyte separates a reference compartment and a test compartment. A potential difference

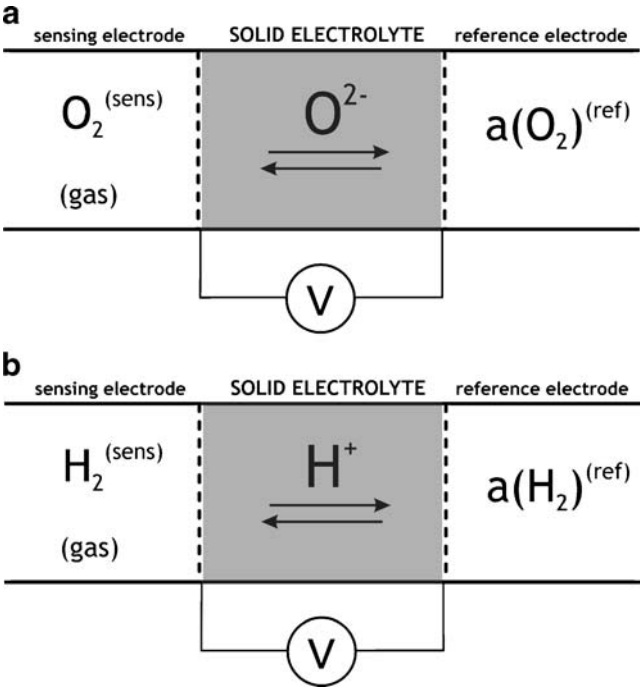

Fig. 1 Schematic illustration of type I potentiometric gas sensor with oxygen conductor (**a**) and protonic conductor (**b**) used as solid electrolytes

is established between the two sides of the solid electrolyte and is dependent on the difference in activity across the solid electrolyte of the species that will equilibrate with the conduction ions in the solid electrolyte. A spectacular example of such sensors is an oxygen sensor with an oxygen-ion conductor, such as cubic zirconia stabilized with yttria [14]. Figure 1a schematically illustrates the sensor structure. The electrodes comprise a porous layer of metal, usually platinum. The electrode reaction, taking place at the three-phase contact points (metal/electrolyte/gas), may be described in the following way:

$$O_{2(gas)} + 4e'_{(metal)} \Leftrightarrow 2O^{2-}_{(electrolyte)} \quad (1)$$

The cell electromotive force (EMF), E, is determined from the Nernst equation:

$$E = \frac{RT}{4F} \ln \frac{p}{p_o} \quad (2)$$

where p and p_o denote oxygen partial pressures at the measuring and reference compartments, respectively. The partial pressure of oxygen at the reference electrode (more precisely oxygen activity), p_o, should maintain constant value. It may be achieved either by passing a gas containing a constant concentration of oxygen (usually air) over the reference electrode compartment or using a so-called 'oxygen buffer.'

The oxygen buffer is a heterogeneous mixture of either a metal, M, and its oxide, MO, (e.g., Pd–PdO, In–In_2O_3, Ni–NiO, etc.) or the mixture of two metal oxides containing

metals of two different valences (e.g., Cu_2O–CuO, CoO–Co_3O_4, etc.).

Taking the Ni–NiO mixture into consideration, as an example, the following chemical equilibrium is established at elevated temperatures (above ca. 1,000 K):

$$NiO_{(s)} \Leftrightarrow Ni_{(s)} + \frac{1}{2}O_{2(g)} \tag{3}$$

From the mass action law for equilibrium (3), we have:

$$p_o = p(O_2) = K_T^2 = \exp\left(-\frac{2\Delta G^o}{RT}\right) = \text{const}|_{T=\text{const}} \tag{4}$$

where K_T and ΔG^o are the equilibrium constant and the standard free enthalpy of the reaction 3, respectively.

The potentiometric hydrogen sensor with a protonic solid electrolyte is another example, important from the viewpoint of practical importance. Figure 1b shows the structure and working mechanism of such sensor.

Most potentiometric hydrogen sensors are based on a new generation of high-temperature proton-conducting materials. The $KTaO_3$-based material was the first one in a series of attempts [15, 16]. Then came acceptor-doped strontium or barium cerates, with the formulas $SrCe_{1-x}M_xO_{3-\delta}$ or $BaCe_{1-x}M_xO_{3-\delta}$, respectively, where M usually denotes a rare earth element, and x is lower than the solubility limit of M^{3+} ions in the crystal lattice (usually less than 0.2). These materials exhibit p-type electronic conductivity under oxidizing atmospheres free from hydrogen-containing gases. In either wet or hydrogen atmospheres, electronic conductivity decreases and the ionic component assumes high values. The studies of potentiometric hydrogen transport revealed that ionic transport is realized by protons. Ionic conductivity is of the order of 10^{-3} to 10^{-2} $\Omega^{-1}cm^{-1}$, within 873–1,273 K. Apart from cerates, protonic conductivity was also reported in zirconate perovskites, although their conductivity is about ten times lower than that of the cerates [17, 18]. High mechanical and chemical stability of zirconates such as $CaZr_{0.9}In_{0.1}O_{3-\delta}$ (with respect to carbonate or hydroxide formation [19]) are the necessary prerequisites for their use in the construction of hydrogen sensors applied in metallurgy [20].

According to the dopant incorporation reaction (Kröger–Vink notation was used), given by Eq. 5:

$$2SrO + Y_2O_3 => 2Sr_{Sr} + 2Y'_{Ce} + 5O_O + V_O^{\bullet\bullet} \tag{5}$$

Trivalent ions Y^{3+} substitute tetravalent Ce^{4+} ions, and an appropriate amount of oxygen vacancies is formed to maintain the electroneutrality condition:

$$x = \left[Y'_{Ce}\right] = 2\left[V_O^{\bullet\bullet}\right] \tag{6}$$

In the presence of either water vapor or hydrogen, protonic defects are formed. Taking into account the small size of protons, we can assume that they do not occupy lattice positions but rather attach to oxide ions, forming OH groups [21]:

$$H_2O + V_O^{\bullet\bullet} + O_O^x \Leftrightarrow 2OH^{\bullet} \tag{7}$$

$$H_2 + 2O_O^x \Leftrightarrow 2OH^{\bullet} + 2e' \tag{8}$$

The formation of OH^- groups has been confirmed by means of infrared method [22, 23].

Protonic defects formed in reactions (7) or (8) ($OH^{\bullet}$) are free to move in the perovskite structure. Barium cerates exhibit the highest total conductivity, but the ionic conductivity component is mixed—both protonic and oxide-ion. On the other hand, strontium cerates show almost purely protonic conductivity [24, 25]. However, both Ba and Sr cerates suffer from instability in CO_2-containing gas atmospheres. In this respect, Ca or Sr acceptor-doped zirconates are much more stable [26, 27].

Acceptor-doped strontium or barium cerates were originally used as a solid electrolyte in humidity sensors [28–32]. They then received interest with regard to hydrogen sensors [32–39].

Iwahara et al. [32, 34] studied the potentiometric cell:

$$\text{Gas I, Pt}|BaCe_{0.90}Nd_{0.10}O_{3-\alpha}|\text{Pt, Gas II} \tag{9}$$

The cell (Eq. 9) worked in a stable manner within the 473–1,173 K range. The sensing signal (EMF) acted according to the Nernst equation. The response time, $t_{0.90}$, corresponding to 90% of the total change of the measured signal, was about 20 s. Despite these satisfactory results, instability in CO_2-containing atmospheres has remained a problem as far as Ba and Sr cerates are concerned. Stability may be improved using a small deficit of barium in respect to stoichiometric composition [36].

Indium-doped $CaZrO_3$ is another example of a potentiometric sensor used to determine hydrogen activity in molten metals [33, 35]. This solution has been used with great success.

A more sophisticated hydrogen sensor composed of a hydrogen pump and a solid cell with $SrCe_{0.95}Yb_{0.05}O_{3-\alpha}$ as the solid electrolyte was proposed by Katahira et al. [37, 38]. The constant hydrogen activity at the reference electrode is maintained here by potentiometric pumping of hydrogen from the measured gas to the reference electrode compartment. The excess of hydrogen is allowed to escape through the calibrated opening.

Figure 2 shows one of the typical sample holders used for the purpose of sensors' measurements. The construction of holder allows separating easily gases at the sensing and reference electrode compartments. Figure 3 shows the example results of the sensor response to the changes of hydrogen partial pressure. The inset in Fig. 3 shows the

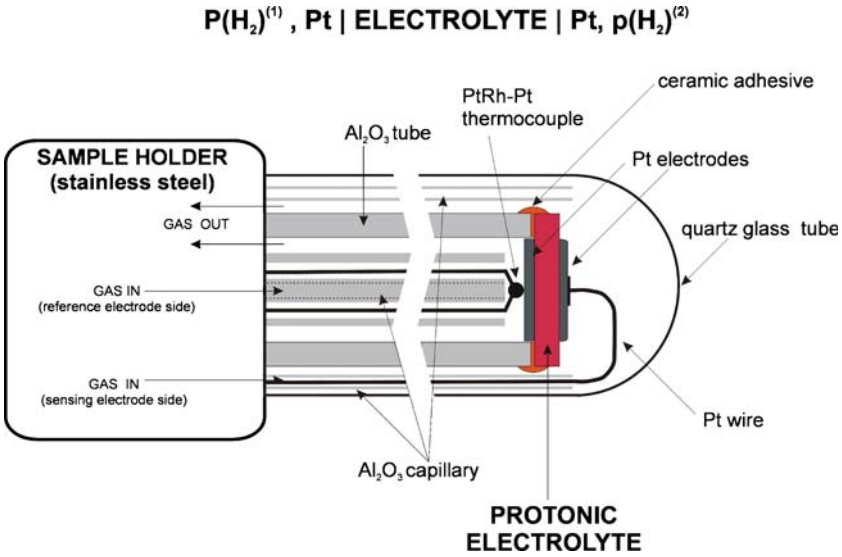

Fig. 2 Sample holder together with the tubular type prototype hydrogen sensor based on protonic conductor, used for the measurements of sensor characteristics

illustration of response time determination. As can be seen, the reversible changes of measured EMF can be observed. The response and recovery times are reasonably short (less than 1 min). Similar results were obtained for sensors based on yttrium-doped strontium cerate and published elsewhere [39].

The other examples of type I potentiometric sensors described in literature are listed in Table 1 [14, 32–44]. As can be seen, the list of type I potentiometric sensors is very short, due to lack of suitable solid electrolytes. There are no solid electrolytes with mobile ions originating from such gases as NO_x, SO_x, or CO_2. The potentiometric sensor of CO_2 with mobile CO_3^{2-} described by Matsumoto et al. [45] could be treated as 'type I', but the electrolyte used was not solid state.

Sensors based on equilibration with the mobile component of solid electrolyte (type II)

In this type of sensors, the gas equilibrates with the component that is different from the predominantly

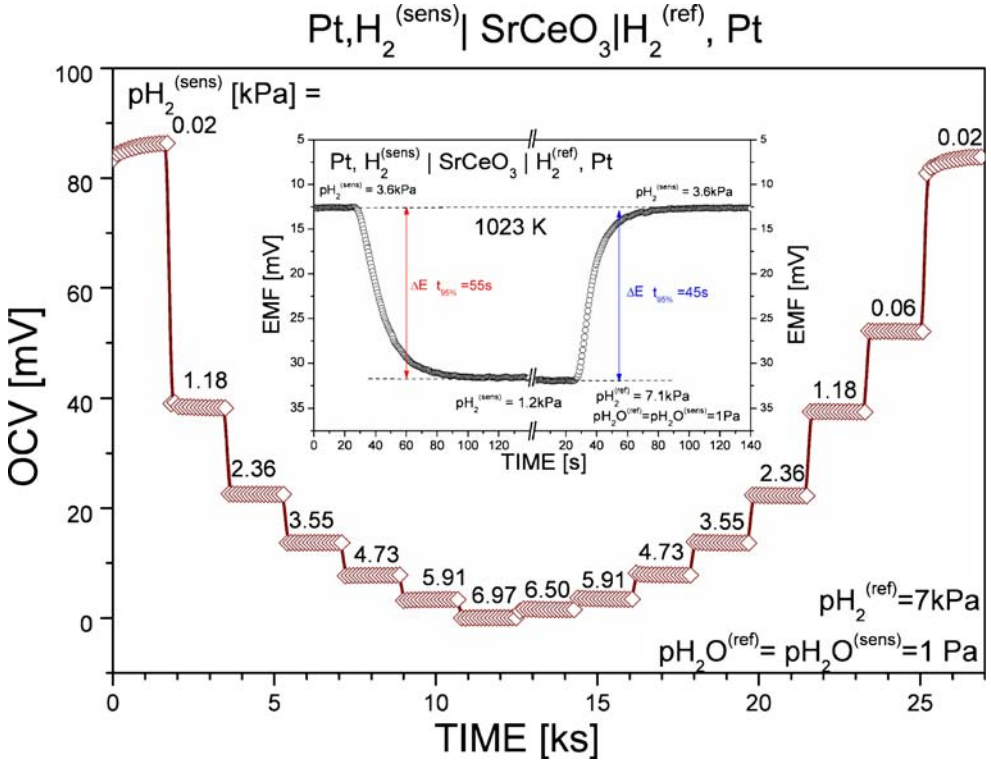

Fig. 3 Dynamic response at 1,023 K of hydrogen potentiometric sensor based on $SrCeO_3$ solid electrolyte. The *inset* shows the example of response time determination of the cell

Table 1 Gas sensors of the type I

Gas	Solid electrolyte	Mobile ion	Reference	Year
O_2	Stabilized zirconia (YSZ)	O^{2-}	[14]	1991
H_2	HUO_2PO_4 $4H_2O$ (HUP)	H^+	[40]	1982
	$SrCe_{1-x}M_xO_{3-\delta}$, $BaCe_{1-x}M_xO_{3-\delta}$; M=Nd, Y, Yb, etc.		[32–39]	1991–2008
F_2	LaF_3	F^-	[41]	1991
Cl_2	$SrCl_2$–KCl	Cl^-	[42]	1999
	$BaCl_2$–KCl		[43]	1997
	$PbCl_2$–KCl		[42, 44]	1999, 1998

mobile species, as shown schematically in Fig. 4. One example is the CO_2 sensor with the K_2CO_3 solid electrolyte, proposed by Gauthier and Chamberland [46].

Let us consider the following solid cell:

$$Pt, O_2, CO_2[p(CO_2 = p_o)] | K_2CO_3 | CO_2 \times [p(CO_2) = p], O_2, Pt \quad (10)$$

In this cell, K^+ ions, the only mobile ions of the solid electrolyte K_2CO_3, interact with gaseous molecules of CO_2, according to the reaction:

$$2K^+_{(electrolyte)} + CO_{2(gas)} + \frac{1}{2}O_{2(gas)} + 2e'_{(metal)} \Leftrightarrow K_2CO_{3(electrolyte)} \quad (11)$$

If oxygen activity is the same at both electrodes, then cell EMF, E, may be expressed as:

$$E = \frac{RT}{2F} \ln \frac{p}{p_o} \quad (12)$$

By replacing the above reference electrode by [46]:

$$Ag_2O|Ag_2SO_4 \text{ in } K_2CO_3 \quad (13)$$

we receive a solid cell, in which EMF:

$$E = \text{const.} + \frac{RT}{2F} \ln p \quad (14)$$

where const. includes the E^o of pure silver sulfate and silver-ion activity in K_2CO_3.

Several examples of type II sensors and their basic parameters are collected in Table 2 [46–54].

Furthermore, NO_x [55] and SO_x [56–59], the type II sensors, are reported.

Surface-modified solid-state ionic sensors (type III)

The application of solid potentiometric cells as gas sensors of type I or II may be successful only in certain cases, i.e., when for the given gas A there exists a suitable solid electrolyte AB with ionic transference numbers—t_A (type I) or t_B (type II)—close to 1. Taking into account other important properties of solid electrolytes, such as the operating temperature range and equilibrium gas pressure, chemical reactivity with metal electrodes and surrounding construction materials, gas-tightness, etc., the list of satisfactory couples (A, AB) is very short, especially for type II.

The application of an additional auxiliary phase, AP, gives a much wider opportunity of applying solid cells as gas sensors [2, 60, 61].

Yamazoe and Miura [13] proposed a further modification of the proposed classification. They divided type III sensors

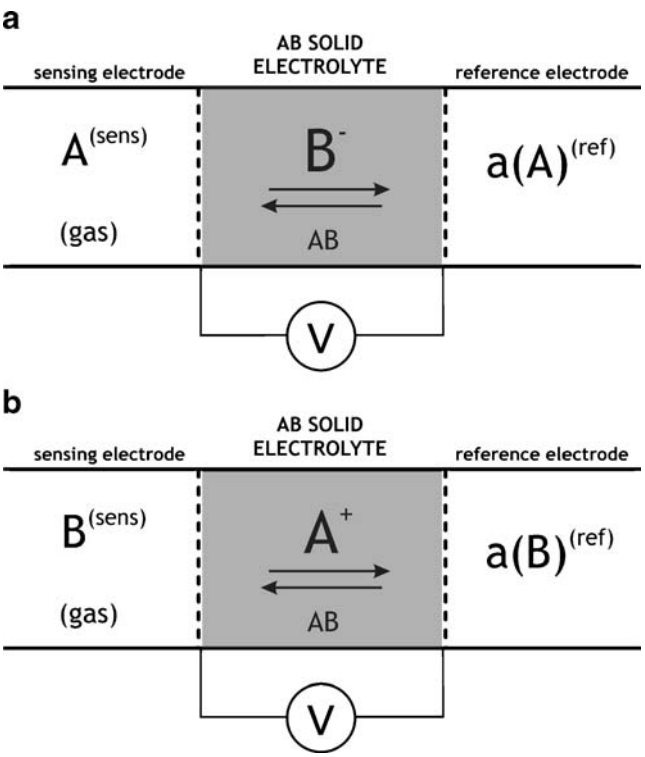

Fig. 4 The illustration of type II potentiometric gas sensor with anion conductor (**a**) and cation conductor (**b**)

Table 2 Performance of electrochemical sensors type II for CO_2

Cell structure *Me*, Ref|SE|Sens|CO_2, O_2 (air) *Me'*[a]	Operating temperature (°C)	Measured concentration (ppm)	Response time (s)	Reference	Year
Ag|Ag_2SO_4 (1 mol% in K_2CO_3)|K_2CO_3|CO_2, O_2, Au	725	50–1,000	Few seconds to few minutes	[46]	1977
	300–750	9–12,000		[47]	1984
Au, CO_2 (p_o), O_2|K_2CO_3|CO_2 (p), O_2, Au	725	1–1,000		[48]	1983
M, CO_2, O_2|Na_2CO_3–K_2CO_3–Y_2O_3|CO_2 (p), O_2, *M*; *M*=Au, Pd, Pt	300–600	1–1,000	1–100	[49]	1997
M, CO_2, O_2|Na_2CO_3–$BaCO_3$|CO_2 (p), O_2, *M*; *M*=Au, Pd, Pt, Ag	580–680	$300–10^5$	0.0045–1,000	[50]	1995
Au, O_2|Ca–ZrO_2|K_2CO_3|CO_2, O_2, Au	750	200–2,000	15	[48]	1983
Au, O_2, CO_2|Li_2CO_3+5 mol% Li_3PO_4)+25 wt% Al_2O_3|CO_2, O_2, Au	300–600	10–1,000	10–30 min	[51]	1995
Pt|$LiCoO_2$–Co_3O_4|Li_2CO_3–Li_3PO_4–$LiAlO_2$ (89:5:6)|CO_2, O_2, Au	350–400	40–1,000	60	[52]	1997
Au|$LiMn_2O_4$|Li_2CO_3+20 wt% MgO|CO_2, O_2, Au	300–405	6×10^3–4×10^4	60–120	[53]	1999
Au, Na_2ZrO_3 + ZrO_2|Na_2CO_3+30 mol% $LiNbO_3$ |CO_2, O_2, Au	450	250–1,000	45	[54]	1999

[a] *Me*, *Me'* Metal; *Ref* reference electrode; *SE* solid electrolyte; *Sens* sensing electrode

into three sub-groups, depending on whether the mobile ions of solid electrolyte, SE, and AP are:

- the same—type IIIa
- different but of the same sign—type III b
- of a different sign—type IIIc

Type IIIa

Figure 5 illustrates the structure of the type IIIa sensor schematically. Let us consider the following cell as an example:

$$M,\ CO_2,\ O_2 \,|\, Na_2CO_3 \,|\, Na^+ - SE \,|\, O_2,\ M' \qquad (15)$$

where *M*, *M'*—metal electrodes, usually Pt, Au, or Pt, Ag.

Na^+–SE—solid electrolyte with Na^+ as mobile ions, such as Na-β″-alumina or NASICON.

Na_2CO_3 plays the role of as the auxiliary phase, AP. The formulation of a theoretical dependence for EMF should start from the chemical reactions taking place at both electrodes.

Sensing electrode

At sensing electrodes involving sodium carbonate, the following reaction is commonly assumed:

$$Na_2CO_3 \rightleftarrows 2\ Na^+ + 1/2\ O_2 + CO_2 + 2\ e' \qquad (16)$$

ΔG_{16} of the reaction 16 may be written in terms of the chemical potentials:

$$\Delta G_{16} = 2\eta(Na^+) + \frac{1}{2}\mu^o(O_2) + \frac{RT}{2}\ln p(O_2) + \mu^o(CO_2) + RT\ln p(CO_2) + 2\eta(e') - \mu^o(Na_2CO_3) \qquad (17)$$

where μ^o and η denote standard chemical potential and potentiometric potential at the sensing electrode, respectively.

Reference electrode

$$2Na^+ + 1/2\ O_2 + 2e' = Na_2O \qquad (18)$$

ΔG_{18} of the reaction 18:

$$\Delta G_{18} = \mu^{o'}(Na_2O) + RT\ \ln a'(Na_2O) - 2\eta'(Na^+) - \frac{1}{2}\mu^o(O_2) - \frac{RT}{2}\ln p'(O_2) - 2\eta'(e') \qquad (19)$$

The superscript ′ denotes reference electrode region, $a'(Na_2O)$ denotes the activity of Na_2O at the Na^+SE/O_2, *M'* interface.

According to the definition of EMF, EMF measurements should be performed when a current flowing across the cell is near to zero, so we can assume that the local equilibria are established on both electrodes. This implies that:

$$\Delta G_{16} = \Delta G_{18} = 0 \qquad (20)$$

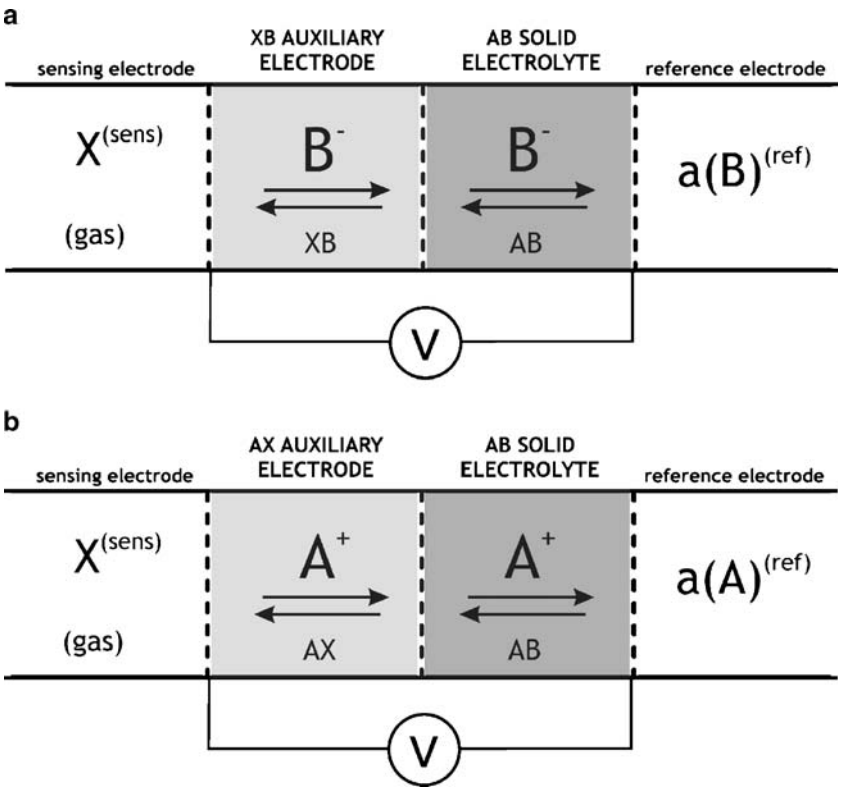

Fig. 5 The potentiometric chain of a type IIIa gas sensor with anion conductor (**a**) and cation conductor (**b**)

Moreover, the difference of the potentiometric potentials of Na^+ ions, $\eta(Na^+)$, at both electrodes is equal to zero because of the good conductivity of Na^+ ions in the Na^+ solid electrolyte:

$$\eta(Na^+) = \eta'(Na^+) \tag{21}$$

Taking into account the general definition of EMF [62] and Eqs. 17, 19, 20, and 21, the following dependence of the electromotive force, E, can be derived:

$$E = -\frac{\eta(e') - \eta'(e')}{F} = \frac{-\Delta G^o(Na_2CO_3)}{2F} + \frac{RT}{2F}\ln\frac{p(CO_2)a'(Na_2O)p(O_2)^{1/2}}{p'(O_2)^{1/2}} \tag{22}$$

where ΔG^o (Na_2CO_3) is the standard free enthalpy of the formation of Na_2CO_3 from Na_2O and CO_2. When oxygen partial pressure at both electrodes is the same, Eq. 22 assumes the form:

$$E = E^o + \frac{RT}{2F}\ln[p(CO_2)a'(Na_2O)] \tag{23}$$

where E^o is the EMF of the cell in standard conditions, and may be expressed as:

$$E^o = -\frac{\Delta G^o(Na_2CO_3)}{2F} \tag{24}$$

As can be seen from Eq. 23, the linear dependence between E and $\ln p(CO_2)$ can be achieved when the activity of Na_2O at the reference electrode is constant:

$$a'(Na_2O) = f(p(CO_2)) = \text{const} \tag{25}$$

Some authors assumed a priori that condition (25) is fulfilled [63–67]; others made efforts to modify the reference electrode in order to achieve this condition.

Weppner et al. [68–70] applied the reference electrode with a constant activity of Na. According to Liu and Weppner [68, 69], the following equilibria are established at the reference electrode containing metallic Na:

$$2\,Na + 1/2O_2 = Na_2O \tag{26}$$

and

$$2Na + O_2 = Na_2O_2 \tag{27}$$

Sodium peroxide, Na_2O_2, is stable below 733 K. Above this temperature, it decomposes to sodium oxide, Na_2O, and oxygen. Applying the Gibbs–Duhem relation to equilibrium (26), we have:

$$\ln a'(Na_2O) = \frac{\Delta G^o_{26}}{RT} - \ln a'(Na) - \frac{\ln p'(O_2)}{2} \tag{28}$$

where ΔG^o_{26} is the standard free enthalpy of reaction (26).

As can be seen from Eq. 28, at constant $p(O_2)$ and the constant activity of sodium, $a'(Na)$, at the reference

electrode, the activity of sodium oxide, $a'(Na_2O)$, also remains constant. The constant activity of sodium can be achieved using either the Na phase [$a'(Na)=1$] [56, 57] or the Na_xCoO_{2-y} phase [59, 71]. The use of Na_xCoO_{2-y} phase makes it possible to construct sensors showing/exhibiting Nernstian behavior.

In order to obtain the constant value of Na_2O activity, Maier et al. [72, 73] proposed the use of the other 'Na_2O buffer' through the application of the heterogenous mixture $Na_2M_xO_{2\times+1} - MO_2$, where M=Zr, Sn, Ti. Below, we present the detailed analysis of the sensing mechanism of the following cell:

$$M, CO_2, O_2, Na_2CO_3|Na^+ - SE|Na_2Ti_6O_{13}, TiO_2, O_2, M' \quad (29)$$

It may be assumed that presented Eqs. 16, 17, and 21 are valid also for cell (Eq. 29). On the other hand, for the reference electrode, the following is true:

$$6TiO_2 + 2Na^+ + 1/2\ O_2 + 2e' = Na_2Ti_6O_{13} \quad (30)$$

Then, ΔG_{30} of the reaction (30) is:

$$\Delta G_{30} = \mu^o(Na_2Ti_6O_{13}) - 6\mu^o(TiO_2) - 2\eta(Na^+) - 2\eta'(e') - \frac{1}{2}\mu^o(O_2) - \frac{RT}{2}\ln p'(O_2) \quad (31)$$

Instead of Eq. 20, we have:

$$\Delta G_{16} = \Delta G_{30} = 0 \quad (32)$$

The combination of Eqs. 17 and 21, as well as Eqs. 31 and 32, leads to the expressions for μ_e, μ_e', and taking into account Eq. 22 we get the following dependence of the electromotive force, E, of the cell:

$$E = -\frac{\eta(e') - \eta'(e')}{F} = \frac{\Delta G^o_{34}}{2F} + \frac{RT}{2F}\ln\frac{p(CO_2)p(O_2)^{1/2}}{p'(O_2)^{1/2}} \quad (33)$$

where $\Delta G^o(Na_2Ti_6O_{13})$ is the standard Gibbs energy of the reaction:

$$Na_2CO_3 + 6TiO_2 = Na_2Ti_6O_{13} + CO_2 \quad (34)$$

When oxygen partial pressures at both electrodes are the same, Eq. 33 takes the form:

$$E = E^o + \frac{RT}{2F}\ln p(CO_2) \quad (35)$$

where E^o is the EMF of the cell in standard conditions and may be expressed as:

$$E^o = \frac{\Delta G^o_{34}}{2F} \quad (36)$$

Type IIIb

Sodium carbonate and the Na^+-conducting solid electrolyte were first applied as the auxiliary phase and the solid electrolyte, respectively, in CO_2 sensors. However, such sensors suffer from high chemical affinity to water vapor. This leads to instability of the sensor signal and to the deterioration of the sensor structure. The use of either lithium carbonate [60, 74] or its mixture with $CaCO_3$ [75, 76] or $BaCO_3$ [77–79] considerably improves stability of the sensor in the presence of water vapor. Replacing sodium carbonate with lithium carbonate gives a new class of potentiometric sensors, classified as type IIIb.

Figure 6 illustrates the structure of type IIIb sensors schematically. A number of type IIIb sensors are known, most of which are designed specifically for the detection of CO_2. Several examples of such sensors and their basic parameters are collected in Table 3 [63, 68, 69, 80–132].

Despite good performance of such sensors, the mechanism of charge transport through the cell is unclear. Ogata et al. [63] studied several CO_2 sensors composed from Na-β-alumina as a solid electrolyte and different auxiliary phases (carbonates of Li, Na, K, Cs and Ca). All sensors show a two-electron mechanism (n=2), but the standard EMF (E^o) reached different values. This suggests that the electrode reactions are similar, but other factors must be taken into account.

There are other possible explanations of the sensing mechanism of type III sensors. For example, for the auxiliary phase composed from Li_2CO_3 (either pure or in a mixture with $BaCO_3$), we can propose the following reactions at the sensing electrode:

$$Li_2CO_3 \rightleftarrows 2\ Li^+ + 1/2\ O_2 + CO_2 + 2\ e' \quad (37)$$

$$Na_2O\ (nasicon)\ =\ 2\ Na\ +\ 1/2\ O_2 \quad (38)$$

$$2Li^+ + 2\ Na\ = 2\ Li\ + 2\ Na^+ \quad (39)$$

Figure 7 shows an example of CO_2 type IIIb sensor characteristics, measured at 748 K. The response time is shown in the inset. As can be seen, the changes of carbon dioxide pressure (line, right axis) are followed by the changes of measured signal, EMF (points, left axis). The determined response time is below 1 min. It is worth to mention that such structure was found to be stable only in a very limited temperature range, close to 740–750 K. At temperatures lower and higher than 740–750 K, sensors exhibit unstable behavior during the long-term exploitation. Such observation can be explained by the formation of liquid phase at the sensing electrode–solid electrolyte interface. More details can be found in [79]. The long-term stability of

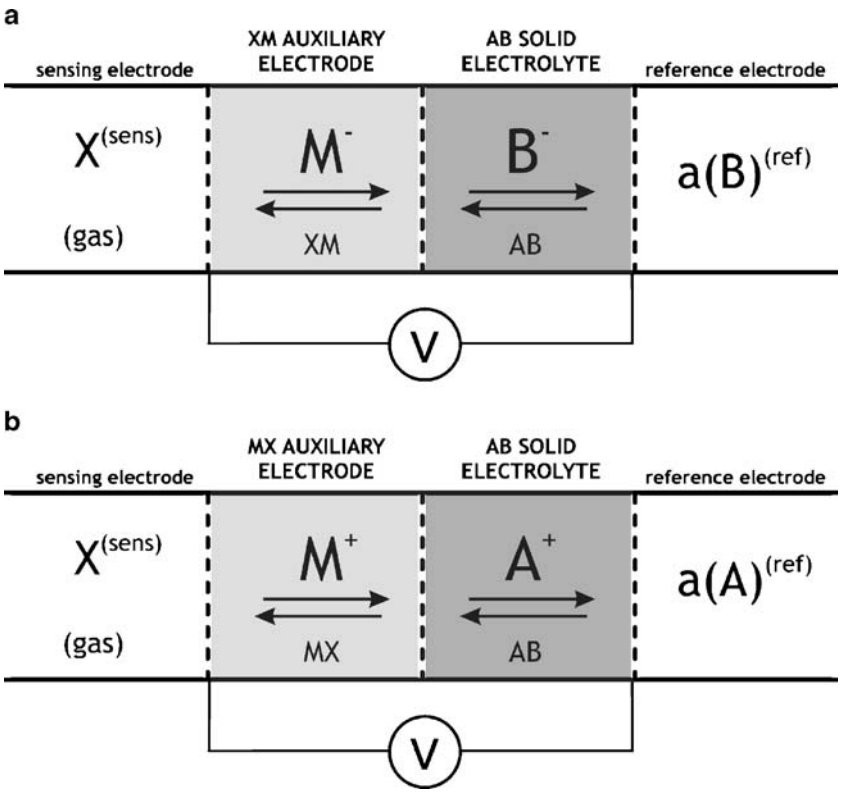

Fig. 6 The potentiometric chain of a type IIIb gas sensor with anion conductor (**a**) and cation conductor (**b**)

any potentiometric sensor is the important problem and wide interdisciplinary issue to be defined and solved in the future. Some selected results related to the problem of long-term stability are presented in [79, 127, 132].

Type IIIc

Figure 8 illustrates the structure of the type IIIc sensors. As an example of the type IIIc sensor, we consider the CO_2 sensor featuring stabilized zirconia as the solid electrolyte and lithium carbonate as the auxiliary phase [76]:

$$\mathrm{Au, air, CO_2}(p) \mid \mathrm{Li_2CO_3} \mid \mathrm{Mg-ZrO_2} \mid \mathrm{air, Pt} \tag{40}$$

The right-hand side electrode serves solely as an oxygen-sensitive reference electrode, at which equilibrium (1) is established, and the left-hand side electrode is the sensing electrode on which the following reaction occurs:

$$2\mathrm{Li}^+ + \mathrm{CO_2} + \frac{1}{2}\mathrm{O_2} + 2e' \Leftrightarrow \mathrm{Li_2CO_3} \tag{41}$$

The auxiliary phase Li_2CO_3 is a Li^+-conducting solid electrolyte. To achieve potentiometric junction between both solid electrolytes, $(O^{2-})Mg–ZrO_2$ and the (Li^+) AP, the formation of an interfacial compound Li_2ZrO_3 containing both conducting ions is postulated. This compound, playing the role of an 'ionic bridge' (IB) between the stabilized zirconia and lithium carbonate, is the product of the reaction:

$$2\mathrm{Li}^+ + \mathrm{O}^{2-} + \mathrm{ZrO_2} \Leftrightarrow \mathrm{Li_2ZrO_3} \tag{42}$$

As follows from equilibrium (42) and Fig. 8, the ionic bridge can play the role of the source or the trap of both cations and anions, depending on cell polarization.

Taking into consideration electrode reactions (1) and (42) and assuming that oxygen partial pressure at both electrodes is the same, the cell EMF, E, may be expressed as:

$$E = E^o + \frac{RT}{2F}\ln p \tag{43}$$

where:

$$E^o = -\frac{\Delta G^o}{RT} \tag{44}$$

and ΔG^o is the standard free enthalpy of the following reaction:

$$\mathrm{Li_2CO_3} + \mathrm{ZrO_2} \Leftrightarrow \mathrm{Li_2ZrO_3} + \mathrm{CO_2} \tag{45}$$

As can be seen from the presented Eqs. 43 and 44, the measured signal E is independent of the parameters of the reference electrode. Moreover, this electrode does not need to be hermetically isolated from the measuring electrode.

Table 3 Performance of electrochemical sensors type III for CO_2

Cell structure *Me*, Ref|SE|Sens|CO_2, O_2 (air) Me′	Sub-type	Operating temperature (°C)	Measured concentration (ppm)	Response time (s)	Reference	Year
Ag|.–Al_2O_3|Me_xCO_3|CO_2, O_2, Ag		400–500	4,000–4.5×10^5		[63]	1986
Me=Li	IIIb			150–280		
Me=Na	IIIa			350–2,000		
Me=K	IIIb			170–1,200		
Me=Cs	IIIb			150–750		
Me=Ca	IIIb			170–900		
Au, O_2|NASICON or β–Al_2O_3|Na_2CO_3|CO_2, O_2, Au	IIIa	320–550	10–4.7×10^4	300	[80]	1987
Pt, O_2|NASICON|Na_2CO_3|CO_2, O_2, Pt		370–520	100–10,000	120	[92]	1993
		450	2–10,000	60	[87]	1992
Pt, Au–Pd, O_2, CO_2|NASICON|Na_2CO_3|CO_2, O_2, Pt		380–450	150–10,000		[106]	1996
Au, O_2|YSZ|NASICONNa_2CO_3|CO_2, O_2, Au	IIIa	520–730	200–5.5×10^5		[80]	1987
		610	100		[84]	1991
Pt, O_2|CSZ (film)|NASICON|Na_2CO_3|CO_2, O_2, Au		560–650	10^4–10^5		[88]	1992
$Na\|Na^+-\beta/\beta''-Al_2O_3\|Na_2CO_3, CO_2, O_2, Pt$	IIIa	150	10^4 to 6×10^5	600	[68]	1990
		450	5–8×10^5	below 60	[85]	1991
$Na\|Na^+-\beta/\beta''-Al_2O_3\|Na_2CO_3, CO_2, O_2, Pt$		150–550	5–8×10^5	60	[69]	1992
Pt, CO_2, $O_2^{\cdot\cdot}$|Li_2CO_3|$Li_{1.3}Al_{0.3}Ti_{0.7}(PO_4)_3$|$Li_2CO_3$, CO_2 (*p*),O_2, Pt	IIIa	650	80–10,000	below 60	[81]	1990
Pt, O_2|NASICON|$BaCO_3$–Na_2CO_3 (1.7:1 mol)|CO_2, O_2, Pt	IIIa	550	4–400,000	8	[82]	1990
					[86]	1991
					[89]	1992
		450–600	250–2,000	8	[90]	1992
Pt, air|NASICON|Li_2CO_3–$CaCO_3$ (1.8:1 mol)|CO_2, air, Pt	IIIb	500	100–100,000	8	[83]	1990
			100–2,000	10–50	[108]	1997
Pt, air|NASICON|Li_2CO_3–$BaCO_3$|CO_2, air, Au		350–600	20–10,000	8	[93]	1993
Pt, air|NASICON|Li_2CO_3–$BaCO_3$|CO_2, air, Pt		350–450	300–5,000	10	[98]	1995
Pt, O_2|ZrO_2-based SE|CO_2, N_2, Pt	IIIc	725–850	5–80% in N_2		[91]	1992
Pt, O_2|Y–ZrO_2|CO_2, N_2, Pt		725–850	5–80% in N_2		[99]	1995
Au,O_2, CO_2|Li_2CO_3+Li_2O|$LiTi_2(PO_4)_3$+0.2 Li_3PO_4|Li_2CO_3+ Li_2O|CO_2 (*p*), O_2, Au	IIIa	650	80–13,000		[94]	1993
				several min	[100]	1995
Pt, O_2|$MgZr_4(PO_4)_6$|M_xCO_3|CO_2, O_2, Pt; *M*=Na; Mg–Ca (1:1)	IIIb	400–500	10–10^6	few min	[96]	1994
Pt, O_2|$Mg_{1.15}$ $Zr_4P_{5.7}$ $Si_{0.3}$ O_{24}|M_xCO_3|CO_2, O_2, Pt, *M*=Na; K		300–500	5,000–6×10^5	below 5 min	[101]	1995
Pt, air (+CO_2)|Mg–ZrO_2|Li_2CO_3|CO_2 (*p*), air, Au	IIIc	400–600	100–1,000	Several tens	[97]	1994
		500–650		10	[102]	1995
Pt, air (+CO_2)|LaF_3|Li_2CO_3|CO_2 (*p*), air, Au		400–450	40–2,000	10–20	[95]	1993
					[103]	1995
Au, O_2, CO_2|(Li_2CO_3+5 mol% Li_3PO_4)+25wt% Al_2O_3|CO_2, O_2, Au		300–600	10–1,000	10–30 min	[104]	1995
$Au, O_2\|Na_2Ti_6O_{13}-Na_2Ti_3O_7(\text{or}-TiO_2)\|Na-\beta/\beta"-Al_2O_3\|Na_2CO_3\|CO_2, O_2Au$	IIIa	500–750	740–9.55×10^5	few s	[98]	1994
					[105]	1995
					[107]	1996

Pt, air|K_2O–Sm_2O_3–6SiO_2|K_2CO_3|CO_2,O_2,Au	IIIa	300–500	10–10,000	240	[109]	1997
Au, $Na_{0.9}CoO_{2-y}$|NASICON|Na_2CO_3|CO_2, air, Au	IIIa	500	10^3–8×10^4	1–40 min	[110]	1998
Pt, O_2|YSZ|Na_2O–Al_2O_3–4SiO_2|Na_2CO_3|CO_2, air, Pt	IIIc	470	10–10^4	2 min	[111]	1998
					[127]	2005
Au|$Li_3Zr_2Si_2PO_{12}$|Li_2CO_3–K_2CO_3–Na_2CO_3|CO_2	IIIb	420	10^3–10^4	15–20 s	[112]	2000
Pt, O_2|YSZ|(β+β″) Al_2O_3|Na_2CO_3|CO_2, O_2, Au	IIIc	400–600	65–10^4	ca. 30 min	[113]	2000
Pt, O_2|YSZ|$Sc_2(WO_4)_3$|Li_2CO_3|CO_2, air, Pt	IIIc	550	200–5×10^4	few min	[114]	2000
					[115]	2001
Au–Pd, O_2|NASICON|Na_2CO_3–$BaCO_3$|CO_2, Air, Pt	IIIa	600–700	250–10^4	several min	[116]	2000
Pt, air|NASICON|Na_3PO_4–$NaHCO_3$–Na_2CO_3|CO_2, air, Au	IIIa	30	300–3,000	5 min	[117]	2001
Au|$LiCoO_2$+5 mol% Co_3O_4|$Li_{2.88}PO_{3.73}N_{0.14}$|$Li_2CO_3$|$CO_2$, air, Au	III a	400, 500	200–3,000	20 s	[118]	2001
					[121]	2003
Au, O_2|$LiFeO_2$–$LiFe_5O_8$|Li^+-glass conducting|Li_2CO_3–Li_3PO_4|CO_2, air, Au	IIIa	500	350–10^5	30 s	[119]	2001
Au, Na_xCoO_2|NASICON|Li_2CO_3–$BaCO_3$+ In_2O_3–SnO_2|CO_2, air, Pt	IIIb	30	300–3,000	below 3 min	[120]	2003
					[128]	2005
Pt, CO_2 (p_o)|$BaCO_3$–Na_2CO_3|Na–β-Al_2O_3|NASICON|CO_2, air, Pt	IIIa	400–600	10^3–10^6	50–70 s	[122]	2003
Pt, air|NASICON|Li_2CO_3–$BaCO_3$|CO_2, air, Au	IIIb	400–500	100–1,000	40 s	[123]	2003
Pt|$Na_2Ti_6O_{13}$–$Na_2Ti_3O_7$ (TiO_2)|NASICON|Li_2CO_3–$BaCO_3$|CO_2, air, Pt	IIIb	300–500	100–12,600	35	[124]	2003
Pt|$Na_2Ti_6O_{13}$–$Na_2Ti_3O_7$ (TiO_2)|NASICON|Na_2CO_3–$BaCO_3$|CO_2, air, Pt	IIIa				[125]	2004
Pt, CO_2 (p_o), air|LISICON|Li_2CO_3|CO_2, air, Pt	IIIa	500	10^3–10^5	Few mn	[126]	2005
Pt, O_2|$Na_2Ti_6O_{13}$–TiO_2|NASICON|Na_2CO_3–$BaCO_3$|CO_2, air, Pt	IIIa	500–600	500–8,000	below 10 min	[129]	2006
Pt|NASICON|Li_2CO_3+Ln_2O_3|CO_2, air, Au	IIIb	460	370–10^4		[130]	2007
Ln=La, Pr, Nd, Sm, Eu, Gd, Y				below 30 min	[131]	2007
					[133]	2008
Au|Li_2TiO_3–TiO_2|Li_3PO_4–SiO_2|Li_2CO_3–$BaCO_3$|CO_2, air, Au	IIIa	450, 500	500–5,000	20–27 s	[132]	2007

Me, *Me′* Metal; *Ref* reference electrode; *SE* solid electrolyte; *Sens* sensing electrode; *CSZ* Cubic Stabilized Zirconia

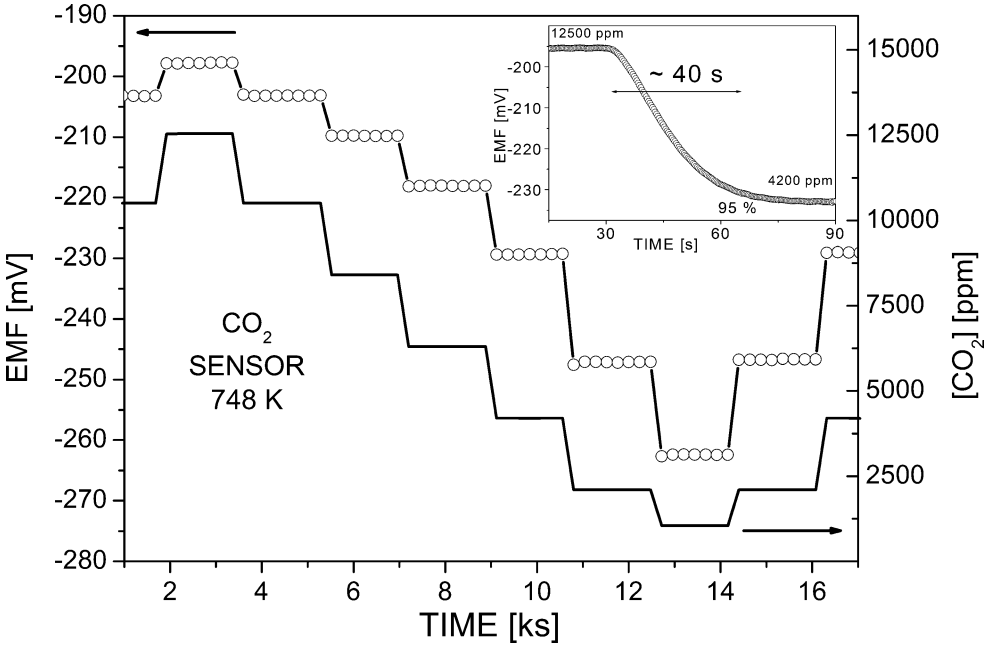

Fig. 7 Transient response at 773 K of type IIIa CO_2 sensor containing Na_2CO_3–$BaCO_3$ and NASICON as the auxiliary phase and the solid electrolyte, respectively. The response time determination of the sensor is shown in the *inset*

This fact gives a huge opportunity to simplify the construction of the sensor. Depending on whether the two electrodes are to be isolated or not, the planar or tubular sensors were proposed (Fig. 9a and b, respectively).

Non-Nernstian behavior of potentiometric sensors

According to the working mechanisms of the potentiometric sensors presented above, the dependence of the sensor signal, EMF, vs partial pressure of the detecting gas, should be in agreement with the Nernst equation (see Eqs. 2, 12, 14, 35, and 43):

$$E = E^o + \frac{RT}{nF}\ln(p \times \alpha) \tag{46}$$

where: p—partial pressure of the detecting gas, α—parameter determining the activity of gas at the reference electrode (e.g., $\alpha = 1/p_o$) and the activity of other species taking part in electrode reactions (see, for example, Eq. 22).

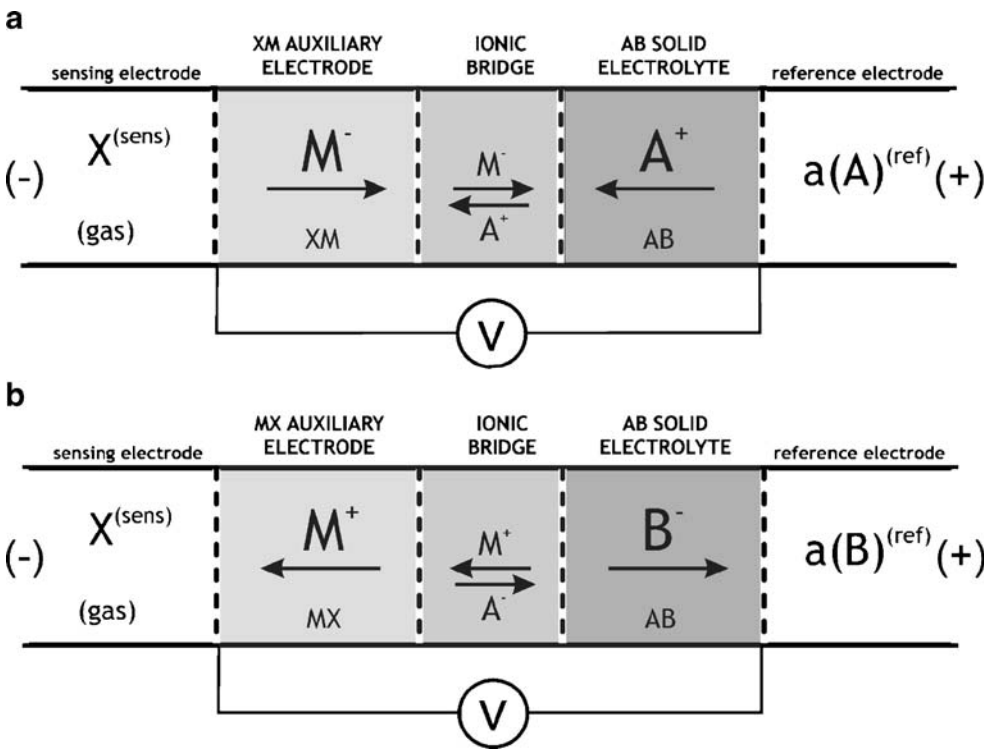

Fig. 8 Potentiometric chain of a type IIIc gas sensor with cation conducting electrolyte (**a**) and anion conducting electrolyte (**b**)

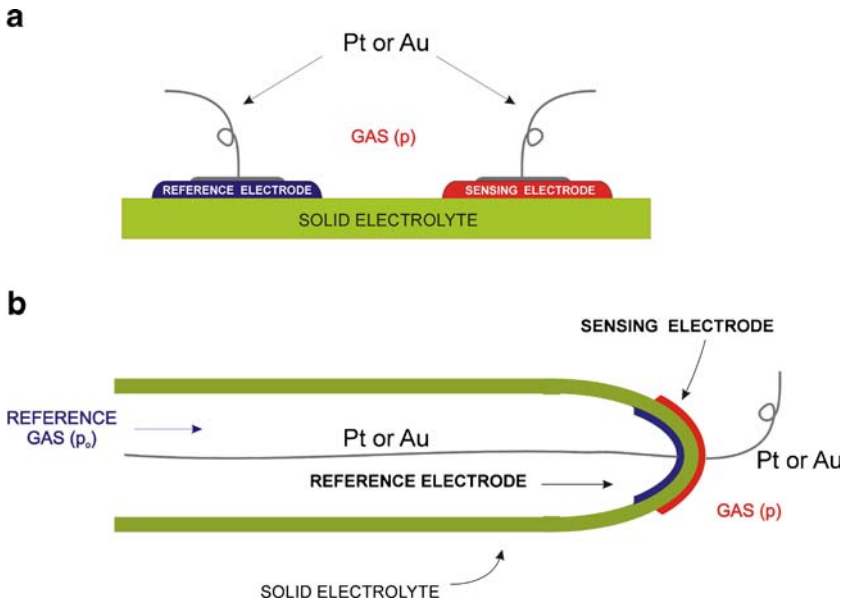

Fig. 9 Structure of planar (**a**) and tubular (**b**) potentiometric sensors

It is worth mentioning that both parameters E^o and n in Eq. 46 exhibit precise physical meaning. Parameter E^o involves free enthalpy of the cell reaction (see e.g., Eqs. 24 and 36), while parameter n should assume an integral value.

However, discrepancies from the theoretically predicted relationship given by Eq. 46 are observed, as illustrated in Fig. 10. The observed discrepancies in the experimental dependencies E vs p from theoretical relationship given by Eq. 46 may be explained in several ways:

- Local equilibria of the reactions which occur at the electrodes, the AP and the IB, are not established. This explanation may be particularly valid at lower operating temperatures. It is to be expected that a gradual change from non-Nernstian to Nernstian behavior with a temperature increase takes place. The observed changes of the parameter n in Fig. 10 remain in agreement with this expectation.
- Two or more competitive potentiometric reactions occur simultaneously at the sensing electrode. This phenomenon is known as 'mixed potential.' This issue will be discussed in greater detail in the next chapter.
- The solid electrolyte exhibits no negligible component of the electronic conductivity. Taking into consideration the following relationship [134]:

$$E_{\text{exper}} = t_{\text{ion}} E \tag{47}$$

where E_{exper} and E denote experimental and theoretical values of the EMF, respectively. According to Eqs. 46 and

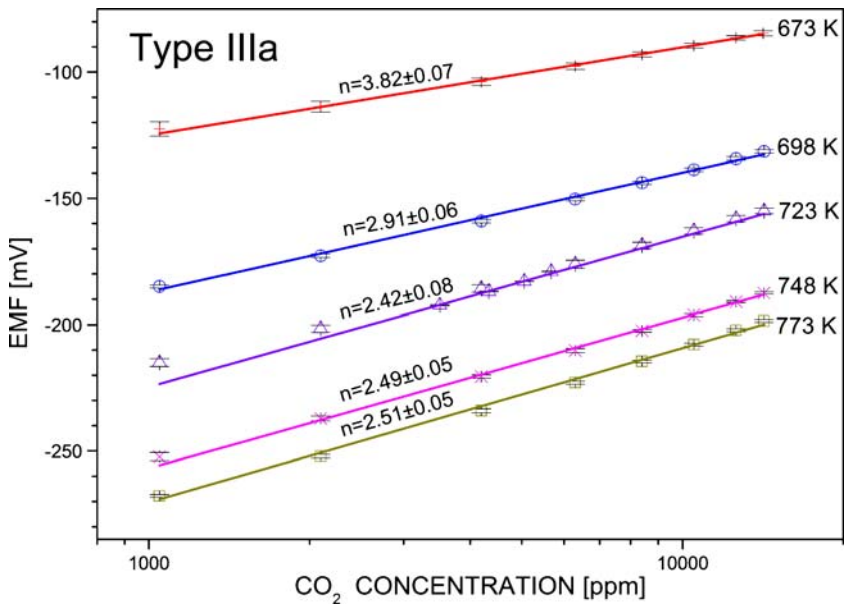

Fig. 10 Experimental dependence of EMF vs $p(CO_2)$ for the CO_2 sensor containing Na_2CO_3–$BaCO_3$ and NASICON as the auxiliary phase and the solid electrolyte, respectively. The determined values of n parameters are given for every measured temperature

47, the experimentally determined parameter n can assume non-integral values. However, Eq. 47 may be treated as only semi-quantitative because it is assumed that the ionic transference number is constant in any place of the solid electrolyte.

A more precise explanation for the EMF behavior was first proposed by Näfe et al. [135–137] for cells with β-alumina as the solid electrolyte. Taking into consideration Näfe's approach, the theoretical values of EMF were calculated for different arbitrarily chosen ionic transference numbers, t' (Na^+). Figure 11 shows the results of calculations for 673 K (Fig. 11a) and 773 K (Fig. 11b) for the sensor as in Fig. 10. As can be seen, even low electronic transference number (5×10^{-3}) leads to the non-Nernstian behavior (n parameter other

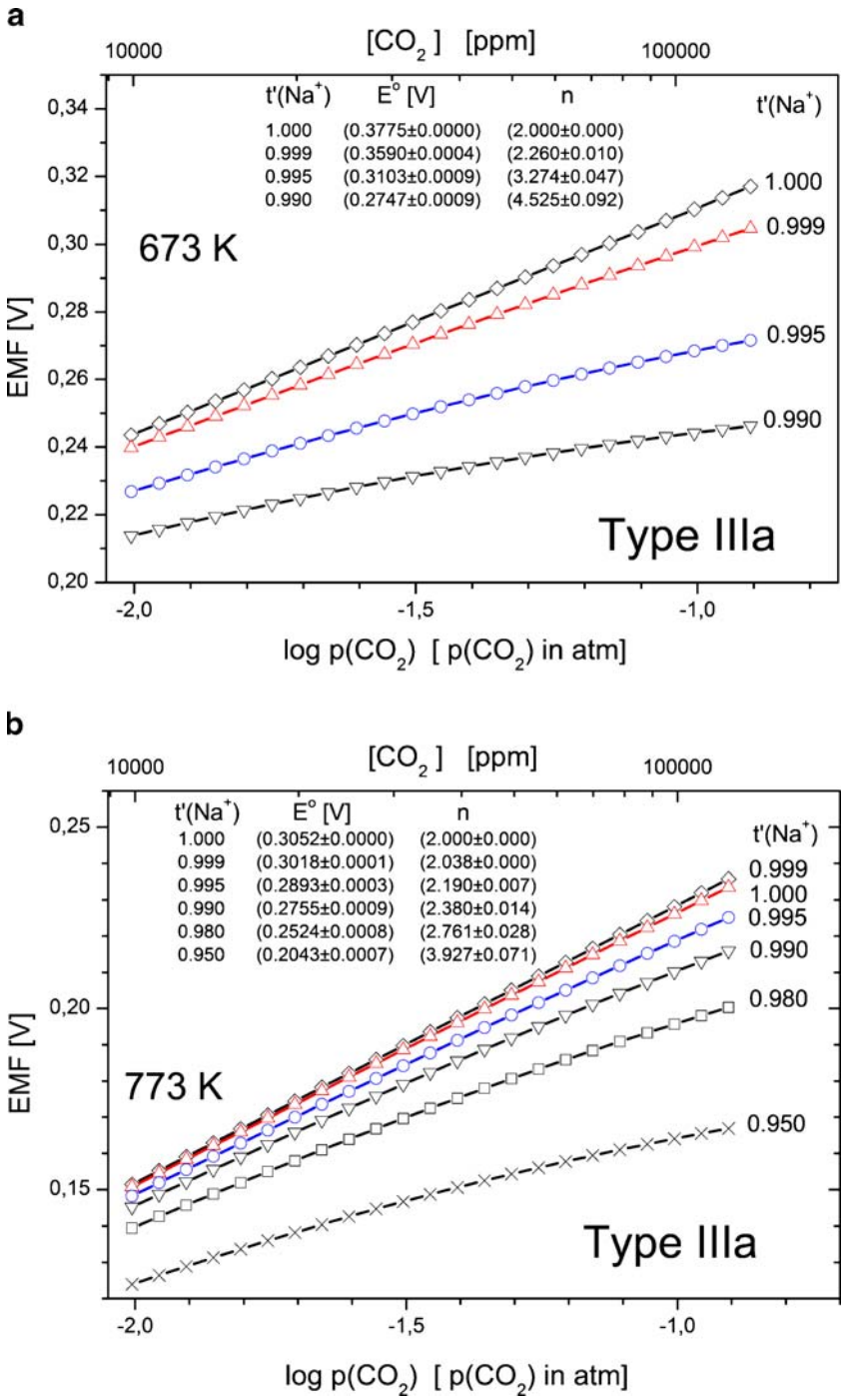

Fig. 11 Theoretical EMF vs p (CO_2) for arbitrarily chosen transference numbers of Na^+ ions at the auxiliary phase–solid electrolyte interface, t'(Na), for 673 K (**a**) and 773 K (**b**). The calculated E° and n parameters for different t'(Na) are also shown

than 2). This influence of electronic transport component is more significant at low temperatures.

- More than one type of ions is mobile in the solid electrolyte. This is expected in particular for hydrogen sensors using high-temperature proton conductors. In that case, both hydrogen and oxygen ions can participate in charge transport through the solid electrolyte [39, 138].
- Surface effects connected with contact potential difference [139].
- There are no negligible interactions between species taking part in electrode reactions. In this case, the activities of the reacting substances instead of their concentrations (expressed in partial pressures) should be placed in Eq. 46.
- The influence of high electrode polarization resistance.

Mixed potential gas sensors

A non-Nernstian behavior of zirconia-based oxygen sensors was first observed by Fleming [140].

He observed a deviation in a theoretically predicted dependence of EMF vs oxygen partial pressure (Eq. 2) in the presence of CO in a gas mixture. According to Fleming, CO may affect sensor performance in two ways. First, CO may decrease the local concentration of oxygen at the sensing electrode as a result of the reaction:

$$CO + {}^1\!/_2\, O_2 = CO_2 \tag{48}$$

Furthermore, there is also a possibility of direct interaction between CO and the sensing electrode:

$$CO + O^{2-} = CO_2 + 2e' \tag{49}$$

This means that apart from the potentiometric reduction given by Eq. 1, the oxidation described by Eq. 49 takes place simultaneously at the sensing electrode. The steady potential of this electrode, known as the mixed potential, is established when the rates of both mentioned reactions are equal. Taking into consideration the fact that both competing potentiometric reactions (1) and (49) take place at a three-phase boundary (named as TPB): gas phase, solid electrolyte, and metallic electrode, their rates are strongly related to chemical composition and microstructure of the electrode, as well as the solid electrolyte. Moreover, the catalytic activity of the electrode material controls the reaction rates and the resulting mixed potential. This was confirmed through experimental work by Wachsman et al. [141, 142]. They concluded that the EMF of the mixed-potential cells is compatible with the changes in the Fermi level induced by chemisorption of the oxidizing or reducing gas in the auxiliary phase, connected to the sensing electrode. However, at present, our knowledge about the working mechanism of this group of gas sensors is rather limited [143–146].

In order to improve the catalytic activity of the sensing electrode towards the detecting gas, several materials have been proposed as the auxiliary phase. Typical examples of the mixed potential sensors several gases are collected in Table 2 of [145]. Some examples not included in [145] are presented in Table 4 [147–168].

Potentiometric sensors for the measurement of environmental gases

Carbon dioxide sensors

Global warming (the green-house effect) has become a serious, worldwide problem that adds to environmental deterioration caused by acid precipitants and the increase of UV radiation due to depletion of stratospheric ozone. The reason for this effect is the emission of gases such as CO_2, methane, freon, and NO_x into the atmosphere. Of those gases, CO_2 has the strongest impact due to the enormous quantity of its emissions into the atmosphere. The most effective way to decrease CO_2 emission is to reduce the amounts exhausted from individual emission sites. For this purpose, the development of simple and inexpensive sensors is vital. Most proposed chemical CO_2 sensors are of the potentiometric type. Those sensors are either type II or III. There are no potentiometric CO_2 sensors of type I, since a solid electrolyte with mobile carbonate anions (CO_3^{2-}) is not known. Several types of potentiometric CO_2 sensors have been reviewed above (Tables 2, 3, and 4). The commercial CO_2 potentiometric sensor is already available; namely, model TGS4160 sensor is produced by Figaro Engineering, Japan.

Nitrogen oxide potentiometric sensors

There is a growing demand for cheap, easy to operate gas sensors for in situ measurements of NO_x (NO and NO_2) in combustion exhausts with regard to the conservation of global environment. Sensors for the detection of NO_x are also useful for analytical purposes, for example in electronic noses, since biological and food processes often produce gas mixtures containing nitric oxide. Nitrogen oxides are known to cause air pollution problems, such as acid rain and photochemical smog, as well as damage to human nerves and the respiratory system. It is mainly emitted from automobiles (especially those using lean-burn and diesel engines), stationary combustion facilities and homes. The NO_x in combustion exhausts is usually present in concentrations of up to several hundred parts per million (the threshold limit values for human exposure are 3 and 25 ppm for NO_2 and NO, respectively [169]). As opposed to nitrogen dioxide, nitrogen

Table 4 Mixed potential sensors

Gas	Cell structure *Me*, Ref|SE|Sens|CO_2, O_2 (air) *Me′*	Operating temperature (°C)	Measured concentration (ppm)	Reference	Year
CO	Pt, O_2|$Ce_{0.8}Gd_{0.2}O_{1.9}$|CO, O_2, Au	550, 600	0–500	[147]	2000
	Pt, O_2|$Ce_{0.8}Gd_{0.2}O_{1.9}$|$LaMnO_3$|CO, O_2, Au	600		[148]	2002
	Pt, air|YSZ|$Y_{0.16}Tb_{0.30}Zr_{0.54}O_2$|CO, air, Au	600, 700	0–500	[149]	2002
	Pt, O_2|Na–β Al_2O_3|Au	250–600	10–200	[150]	2004
	Au, air|YSZ|WO_3, +$LaFeO_3$|CO, air, Au	550–650	20–1,000	[151]	2005
	Pt(Au), CO, O_2|YSZ|Nb_2O_5|CO, O_2, Pt (Au)	450–650	1,000	[152]	2008
CO_2	Pt, $La_{0.8}Pb_{0.2}CoO_3$|NASICON|$NdCoO_3$|CO_2, O_2|Au	200–300	100–2,000	[153]	2000
	Pt, $La_{1-x}Sr_xMnO_3$|NASICON|Na_2CO_3–Ba(Sr)CO_2|CO_2, O_2|Au	150–500	$1–10^4$	[154]	2003
NO_x	Au, air|YSZ|WO_3, +$LaFeO_3$|NO_2, air, Au	550–650	20–1,000	[155]	2004
				[156]	2005
	Pt, O_2|YSZ|$(Al_{0.2}Zr_{0.8})_{20/19}Nb(PO_4)_3$|$(Gd_{0.9}La_{0.1})_2O_3$–$LiNO_3$|NO, air,Au	250	200–2,000	[157]	2005
	Pt, O_2|ZrO_2+8 mol% Sc_2O_3|CuO+$CuCr_2O_4$|NO_2, O_2, Pt	518–659	10–500	[158]	2006
	Pt, O_2|YSZ|$ZnFe_2O_4$|NO_x, Pt	600–700	50–450	[159]	2004
H_2S	Au|NASICON|Pr_6O_{11}–SnO_2|H_2S, air, Au	200–400	6–50	[160]	2007
CH_x	Pt, air|YSZ|In_2O_3+MnO_2|CH_x, O_2, Au	600	0–500	[161]	2003
	Pt, air|YSZ|$SrCe_{0.95}Yb_{0.05}O_{3-y}$|$CH_x$, O_2, Au	600	0–1,000	[162]	2001
	Ag|Ag_2O|α-$Zr(HPO_4)_2$|CH_x, air, Pt	200–300	0–100	[163]	2001
	Au, N_2|Al.–Na_3PO_4|CH_4, Au	600	1×10^4 to 3×10^4	[164]	2002
	Pt, O_2|YSZ|$La_{0.8}Sr_{0.2}CrO_3$|C_3H_6, N_2, Pt	500–600	0–1,250	[165]	2003
	Au, O_2|YSZ| $La_{1-x}Sr_xCr_{1-y}Ga_yO_{3-\delta}$|$CH_x$, Au	600–800	$0–8\times10^3$	[166]	2004
	CH_x=C_3H_6, C_3H_8, C_7H_8 (toluene)			[167]	2004
	Au|Na_2CO_3|Na–ZSM–5 (SiO_2/Al_2O_3=27)|C_3H_8, O_2,Au	400	200–4,000	[168]	2006

Me, *Me′* Metal; *Ref* reference electrode; *SE* solid electrolyte; *Sens* sensing electrode; Na-ZSM-5 – Na^+ ion conducting zeolite (aluminiumsilicate)

oxide is not highly toxic, but it has a strong impact on the destruction of stratospheric ozone [170]. The gas composition of NO_x is determined by temperature and $p(O_2)$. Figure 12 illustrates the equilibrium composition of a NO_x gas mixture as a function of temperature at several $p(O_2)$.

Measurements of NO_x concentration have so far been done by means of spectroscopic instruments based on chemical luminescence or infrared absorption. However, such instruments cannot fit well in on-site feedback control systems because of time-consuming analytical procedures, bulky size, and high costs. It is beyond any doubt that only a gas sensor which could determine the concentration of NO_x within a range required by a particular application, with precision and negligible cross-sensitivity to other gases present in studied

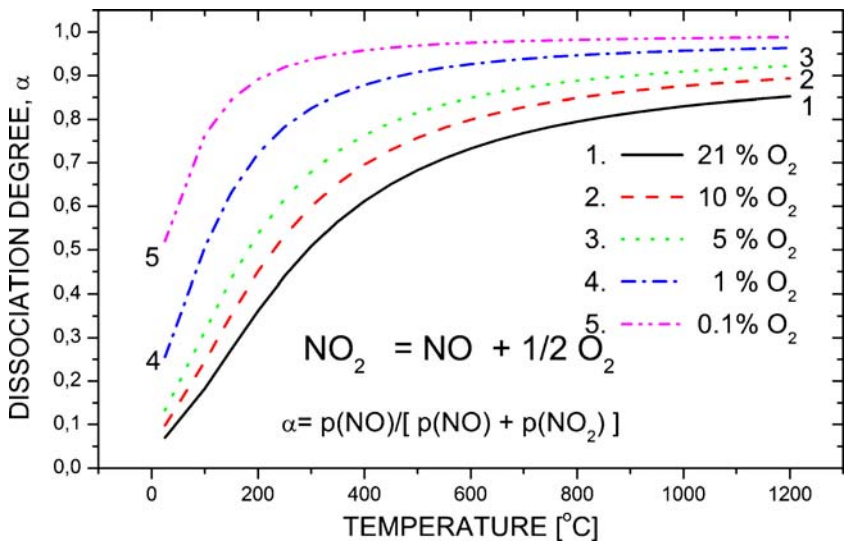

Fig. 12 Equilibrium composition of NO_x gas mixture as a function of temperature at several $p(O_2)$

gas phase, may satisfy the growing demands of modern technology and environmental protection.

Since Gauthier and co-workers reported the possible use of an alkali sulfate-based gas sensor for detecting SO_2 gases in air [46], potentiometric gas sensors for other gases have been reported, with similar principles of operation. Among them, the potentiometric NO_x sensors were also reported [171–192]. The potentiometric NO_x gas sensor has the following solid-cell structure:

$$\text{air, Me}|\text{SE}|\text{AP}|\text{Me, air, NO}_x \quad (50)$$

where Me—metallic connections, usually Pt or Au, SE—solid electrolyte, AP—the auxiliary phase.

NASICON [173, 175, 176, 181], sodium β/β″-alumina [172–174], Ag β/β″alumina [171], and stabilized zirconia [179] were used as solid electrolytes. As the auxiliary phase, simple barium nitrate [46], sodium [174], silver [171], and sodium nitrite [174] have been proposed at the very beginning. The replacement of nitrate phase with nitrite improves NO_2 sensing characteristics and decreases the detection limit (to about 0.2 ppm) [183]. However, the low melting points of these salts (Table 5 [183]) imposes some limitations on the selection of suitable solid electrolytes and working temperatures of the sensor.

As can be seen from Table 5, the operation temperature in the case of $NaNO_3$ as the auxiliary phase should be lower than 307 °C. In addition, in that case, the sensor is incapable of NO detection. Higher temperature operation is achieved through the use of $Ba(NO_3)_2$ as the auxiliary sensing electrode [175]. Using more complex phases such as $NaNO_2$–Na_2CO_3 [184] or $NaNO_2$–Li_2CO_3 [100], the performance of the sensor, especially with diluted NO_2, may be improved.

Assuming that we have a Na^+ ionic conductor (e.g., NASICON or $Na-\beta-$alumina) as the solid electrolyte and $NaNO_3$ as the auxiliary phase, the electrode reactions may be expressed in a way similar to that shown for CO_2 sensors.

Table 5 Melting point of several nitrates and nitrites

NITRATES		NITRITES	
Formula	Melting point (°C)	Formula	Melting point (°C)
$LiNO_3$	264	$LiNO_2{\cdot}H_2O$	>100
$NaNO_3$	307	$NaNO_2$	271
KNO_3	334	KNO_2	440
$Mg(NO_3)_2.\ 2H_2O$	129	$Mg(NO_2)_2{\cdot}3H_2O$	d100
$Ca(NO_3)_2$	561	$Ca(NO_2)_2{\cdot}H_2O$	d100
$Ba(NO_3)_2$	592	$Ba(NO_2)_2$	d217
$AgNO_3$	d444	$AgNO_2$	d140

d Decomposes

Hence, the reactions at the sensing electrode are [175]:

$$Na^+ + NO_2 + Na_2O_2 + e' = NaNO_3 + Na_2O \quad (51)$$

and:

$$Na^+ + NO + Na_2O_2 + e' = NaNO_2 + Na_2O \quad (52)$$

while the counter electrode reaction is:

$$Na_2O\ (\text{from the solid electrolyte}) = 2Na^+ + {}^1/_2\,O_2 + 2e' \quad (53)$$

So, under the constant $p(O_2)$, we have:

$$E = E^o + \frac{RT}{F}\ln[p(NO_2)\ \text{or}\ p(NO)] \quad (54)$$

Similar processes may be proposed for other cation-conducting solid electrolytes like Ag- or Ba-β″-alumina (mobile Ag^+ or Ba^{2+} ions, respectively) or $BaZr_4P_6O_{24}$ (Ba^{2+} mobile ion). Slightly different processes have been proposed for anion-conducting solid electrolytes as LaF_3 (F^- mobile ion) or Y–ZrO_2 (O^{2-} mobile ion). The latter case was considered by Kurosawa et al. [180]. These authors investigated the following solid cell:

$$\underset{\text{(reference electrode)}}{\text{air, Pt}} \;|\; \underset{(O^{2-}\text{conductor})}{\text{MgO}-\text{ZrO}_2\ (\text{MSZ})} \;|\; \underset{\text{(auxiliary phase)}}{\text{Ba(NO}_3)_2} \;|\; \underset{\text{(sensing electrode)}}{\text{Au, NO}_x + \text{air}} \quad (55)$$

The authors postulated that a compound containing both Ba^{2+} and O^{2-} is formed at the phase interface between MSZ and $Ba(NO_3)_2$, according to the reaction:

$$Ba^{2+} + O^{2-} + ZrO_2 = BaZrO_3 \quad (56)$$

At the sensing electrode, the following reactions were suggested:

$$Ba^{2+} + 2NO_2 + O_2 + 2e' = Ba(NO_3)_2 \quad (57)$$

$$Ba^{2+} + 2NO + 2O_2 + 2e' = Ba(NO_3)_2 \quad (58)$$

By combining Eqs. 56 and 57 or 56 and 58, we have a resulting electrode reaction. For example, in the case of NO_2 gas sensing, we get:

$$BaZrO_3 + 2\,NO_2 + O_2 + 2e' = Ba(NO_3)_2 + O^{2-} + ZrO_2 \quad (59)$$

The formed oxygen ions at the sensing electrode diffuse through the MSZ solid electrolyte to the reference electrode, where the following reaction occurs:

$$O^{2-} = 1/2\ O_2 + 2e' \quad (60)$$

A conventional approach to the electrode equilibria (Eqs. 59 and 60) leads to the following expression for EMF:

$$E = E^o + \frac{RT}{F}\ln[p(NO_2)] + \frac{RT}{4F}\ln\frac{p(O_2)^{(s)}}{p(O_2)^{(r)}} \quad (61)$$

where $p(O_2)^s$ and $p(O_2)^r$ denote partial pressures of oxygen at sensing and reference electrodes, respectively.

The mechanisms of particular sensors, described above, ignore the role of chemisorption phenomena on sensor operation. Due to the chemisorption of even very diluted gases from the surrounding atmosphere, a drastic change in the EMF of zirconia oxygen gas sensor [185] takes place. Miura et al. [185, 186] reported the results concerning several materials suitable for use as auxiliary phases. Among 12 kinds of spinel-type oxides tested, $CdMn_2O_4$ was found to be the best material for NO_x sensing. The following sensor with $CdMn_2O_4$:

$$\text{air, Pt}|\ \text{YSZ}|\ CdMn_2O_4,\ \text{Pt, } NO_x, \text{ air} \quad (62)$$

showed excellent response characteristics to both NO (up to 600 ppm) and to NO_2 (up to 200 ppm), at temperatures 500 and 600 °C. The EMF of the device was an almost linear function with the logarithm of NO and NO_2 concentration, with negative and positive slopes for NO and NO_2, respectively. The sensing mechanism involving mixed potential was derived from the polarization curves.

At the reference electrode, the equilibrium described by Eq. 60 is established, while at the sensing electrode, there is the following local equilibrium:

$$2NO + 2\ O^{2-} = 2\ NO_2 + 4\ e' \quad (63)$$

An interesting attempt has been made with regard to this matter in the development of a thick-film ZrO_2-based sensor [192]. The principle of operation of this sensor is based on the removal of an amount of decomposed oxygen which is proportional to that of NO. The problem with this indirect detection is that a certain optimal oxygen partial pressure should be maintained for the decomposition to occur. This requires simultaneous monitoring of the ambient $p(O_2)$ level. In spite of the linear output characteristics of the sensor and a wide measuring range of NO concentrations (0–2,000 ppm) at temperatures up to 700 °C, this sensor suffers from a high error of measurement (ca. 8%) and still needs sufficient improvements. As mentioned above, zirconia-based sensors are versatile with regard to material selection and device construction, and by designing the auxiliary phase or sensing electrode appropriately, they can be upgraded to show excellent sensing performance under specific conditions. With these attractive features, this group of NO_x sensors appears to be the one best suited to sensing not only NO_x but also other oxygenic gases. Unfortunately, there are still many problems related to these devices [13]. Some of them are as follows:

1. It has been proven that, in many NO_x sensing devices, the EMF is totally independent of the coexisting $p(O_2)$ and is inconsistent with the electrode reactions so far assumed. The participation of peroxides or some excess oxygen is suspected.
2. The materials for the auxiliary phase or sensing electrode, mostly composite, have so far been developed empirically. The structure and properties of these materials should be characterized carefully in order to establish guidelines for the design of auxiliary phases. Regretfully, we have no reliable criteria for finding and predicting the most useful materials for individual applications.
3. The sensitivity of sensors with mixed potential depends on the chemisorption properties of the auxiliary phase used. In order to improve the basic parameters of such sensors, knowledge about the interface properties of the applied materials is essential.

Mixed potential NO_x sensors were recently the subject of review papers [193, 194]; some examples of such sensors are also collected in Table 4.

Sulfur oxide sensors

Recently, several potentiometric SO_x sensors of type II have been proposed. They used the following metal sulfates, e.g., K_2SO_4 [195–197], Na_2SO_4 [53, 198], Li_2SO_4 [199, 200], Ag_2SO_4 [201, 202], and Li_2SO_4–Ag_2SO_4 [201, 203, 204] as solid electrolytes. In order to improve sensor characteristics caused by undesirable properties of the used solid electrolytes (phase transformations [205–207] and their low electrical conductivities), more complex sulfate systems and some non-sulfate additions were used, e.g., Na_2SO_4–$Y_2(SO_4)_3$–(–Li_2SO_4) SiO_2 [47, 138], Na_2SO_4–$La_2(SO_4)_3$–Al_2O_3 [208, 209], Na_2SO_4–$NaVO_3$–$Ln_2(SO_4)_3$ (Ln=Eu, Pr, Y) [210].

There are also some known type III SO_x sensors using Na(Ag)-β″-alumina [211–215], or NASICON [216–219] as solid electrolytes. These sensors are without any auxiliary phase added intentionally. However, the detailed studies of the phase composition of these sensors revealed that Na_2SO_4, which plays the role of the auxiliary phase, is formed at the surface of the Na-conducting solid electrolyte through its direct reaction with gaseous SO_2 and O_2 [220]. The sensors containing both the solid electrolyte and the auxiliary phase (added intentionally) are described in [221]

(NASICON/Na_2SO_4) and [222] Lalauze and Rekas (unpublished; β-Al_2O_3/Na_2SO_4).

The principle of SO_x detection with these solid electrolytes was comprehensively described in various papers [223, 224]. These sensors repeatedly responded well to SO_x, but they appeared to suffer from sluggish responses and from the chemical instability of the solid electrolytes in atmospheres containing SO_x. Furthermore, all the sensors reported to date require an independent determination of $p(O_2)$ in order to independently calculate the concentrations of both SO_2 and SO_3.

More recently it has been found that a stabilized ZrO_2 tube coated with K_2SO_4 [194] or Li_2SO_4–$CaSO_4$–SiO_2 [223, 225, 226] as auxiliary phases, can be utilized as an SO_x sensor with a reasonably good response and a stable output. However, both the chemical and mechanical stability of these sensors proved poor during extensive tests. Furthermore, these sensors have a working temperature range restricted to 600–800 °C and are still far from meeting the industry demands for a reliable sensor [13].

From a practical point of view, no work has been done on a solid-state sensor that would measure SO_x concentration under industrial conditions. Instead, most investigations have been focused on potentiometric sensors which measure equilibrium SO_x concentration in air, from which the SO_2 concentration is then calculated from the equilibrium constant of the reaction [227]:

$$SO_2 + \frac{1}{2}O_2 \Leftrightarrow SO_3 \tag{64}$$

The most attractive SO_3–SO_2 solid electrolyte sensor has the following properties and features [224]:

- operation temperature in the range 800–1,200°C
- in situ operation with no umbilical tubing
- no external housing or gas train
- no external reference
- no gas-handling systems
- manifold operation for process control
- no internal seal between measuring and reference electrodes
- no filters for particle-loaded gases

Not a single sensor from those described above can match all these stringent commercial requirements at the same time.

Further development of SO_x sensors has been based on the fact that the zirconia electrolyte should be combined with the composition of the metal sulfates, which plays the role of the auxiliary phase. As follows from the considerations given above (type IIIc), these SO_x sensors need an interfacial compound between the stabilized zirconia and the auxiliary phase to establish a potentiometric chain though the sensor ('ionic bridge'). Furthermore, the results indicated that the output EMF and the sensitivity of sensor depend not only on the properties of the two gas electrodes but also on the thermodynamic properties of the interfacial compound (see Eq. 44). This suggests that the sensors which have a poor interfacial compound between the zirconia and the metal sulfate have unstable behavior and tend to show sluggish responses to SO_x. This tendency became more obvious as the concentration of SO_x increased [228].

Carbon oxide potentiometric sensors

Carbon monoxide is produced by incomplete combustion. It is commonly found in the exhaust gases from engines or as a product of incorrectly adjusted gas heaters. CO is highly toxic, rendered all the more dangerous by its colorless and odorless character. The development of solid-state CO sensors is therefore very desirable. So far, there have been many reports on CO sensors. Most of them concern semiconductor-type CO sensors, which use mainly SnO_2. However, such devices have significant disadvantages, e.g., high cross-sensitivity to other reducing gases or humidity and poor long-term electrical stability. Moreover, such sensors require laborious calibration, since their electrical conductivity is a complex function of microstructure, chemical composition, mutual relations between surface and bulk properties, and geometrical dimensions.

There is hope that these difficulties may be overcome through the development of potentiometric CO sensors. The first attempts at such sensors were amperometric and used liquid [229] or solid organic [230] electrolytes and, finally, yttria-stabilized zirconia with an attached catalyst layer for the oxidation of CO [231]. Recently, potentiometric zirconia-based sensors have also been proposed [231–238]. According to [235], the use of oxide electrodes with stabilized zirconia, based on a mixed-potential model, is an active and very selective way of detecting CO. The combination of CdO and SnO_2 as electrodes yields an excellent CO sensor. Operating at high temperatures such as 600 °C, this sensor shows very promising sensing characteristics. The times of 90% response of the sensor and the recovery to 200 ppm CO at 600 °C were as short as 8 and 10 s, respectively. The EMF value was linear with the logarithm of CO concentration in the range of 20 to 4,000 ppm. Moreover, the cross-sensitivities to other gases such as H_2, NO, NO_2, CO_2, O_2, and H_2O were small or insignificant [230]. Fortunately, it is noted that the EMF value of the sensor was almost independent of the oxygen concentration in the tested range of 2–21 vol%. The detailed sensing mechanism, long-term stability, and simplification of the sensor are now under investigation.

Another composition of a mixed electrode was proposed by Sorita and Kawano [237, 238]. Using $LaMnO_3$ with

yttria-stabilized zirconia oxide (YSZ), they constructed a CO sensor working at 400 °C, within 500–7,000 ppm, and a response time of less than 10 s.

Some examples of the potentiometric CO sensors are collected in Table 4. Recently, Fergus [239] has presented the review concerning potentiometric CO sensors.

Hydrocarbon potentiometric sensors

The presence of hydrocarbons in the atmosphere is a potential hazard in many industrial, commercial, and domestic environments. Since hydrocarbons, and mainly methane, are a product of decaying organic matter, they are also found in dangerous quantities in mines, sewers, and waste tips. Most proposed hydrocarbons sensors are either semiconducting (Taguchi Gas Sensors) or microcalorimetric (pellistors).

Hibino et al. [240] proposed a sensor for detecting CH_4 in exhaust gases from gasoline engines. It was constructed from two Pd (porous)|Y–ZrO_2|Au cells, which are attached to each other with their Pd electrodes on the interior side of the assembly. It was proved that CH_4 reacts with O_2 (below 200 ppm) or H_2O (above 200 ppm) on the Pd electrode and that it barely reacts at all on the Au electrode. When sample gases consisting of CH_4, O_2 and H_2O were fed to the sensor at 750 °C, EMF values were generated from one cell and then compensated by potentiometricly pumping O_2 from the other cell. The current applied to the latter cell increased linearly with methane concentration but was not influenced by changing O_2 concentration. This sensor can determine CH_4 concentrations from 50 up to 700 ppm. Recently reported mixed potential hydrocarbon sensors are collected in Table 4 and these are in review paper [239]. However, further investigations are needed to specify the sensing characteristics and long-term stability of such sensors.

Conclusions

The progress in the research and development of potentiometric sensors in the recent years has been very rapid, as research groups made great efforts to make accurate and reliable in situ measurements of various components in gas phases such as O_2, H_2, CO_2, SO_x, NO_x, CH_x, CO, etc. possible.

Generally, potentiometric gas sensors are characterized by high sensitivity and selectivity, as well as long-term stability. The sensitivity and selectivity of those sensors is affected by electrode redox reactions and by rates of simultaneous reactions occurring at electrodes (in the case of mixed potential). Usually, the sensing signal, i.e., the open cell voltage (the equivalent of the EMF), shows a logarithmic dependence on the gas concentration. This makes it possible to analyze the gas in a wide range of concentrations. An appropriate selection of electrode materials enables the construction of a planar-type cell with sensing and reference electrodes placed in the same compartment and exposed to the same atmosphere. Finally, these sensors can be manufactured in a reproducible manner, thus eliminating the need for expensive individual calibration.

According to the original works on potentiometric sensors, they showed Nernstian behavior. Further studies revealed smaller or larger deviations from the Nernst law. This discovery led to the introduction of a new class of potentiometric sensors, known as mixed-potential sensors. The operation of mixed-potential gas sensors is based on heterogeneous catalytic phenomena. Consequently, enormous so-far knowledge of the heterogenous catalysis in general and semiconductor chemisorptive gas sensors in particular may be used in order to further develop this class of potentiometric sensors.

However, there are still many problems which need solutions. For example, sensor parts, both solid electrolyte and electrode materials, have frequently been chosen empirically. More general rules or principles of their selection should be established to obtain better sensor parameters. In particular, we need further basic studies on the catalytic activity of both chemical and potentiometric reactions taking part in the sensor. Moreover, further studies are required to better understand the sensor mechanism.

The sensors may be used in a variety of areas, including domestic applications, agriculture, industry, medicine, automobiles, mines, control of gas emissions, leak, fire, etc. Low costs of manufacture, easy maintenance, and small dimensions of the sensors offer the possibility of installing them in many places. As a result, it will be possible to correct control gas atmosphere and to optimize various industrial processes. Other applications for potentiometric sensors still need to be explored.

Acknowledgement The financial support of Polish Ministry of Science and Higher Education (MNiSW), Projects No. 3T08D04929 and K133/T02/2006 (PBZ-KBN-117/T08/03) is acknowledged.

References

1. Göpel W (1985) Tech Mess 52:47 (in German)
2. Weppner W (1987) Sens Actuators 12:107
3. Gulyurtlu I, Lopes H, Cabrita I (1996) Fuel 75:940
4. Ayers GP, Granek H (1997) Clean Air 31:38
5. Kakaras E, Vourliotis P (1995) J Inst Energy 68:22
6. Lunt R, Little AD (1996) Chem Eng Progress 2:11
7. Daly L (1998) What's New in Process Eng 3:59
8. Wigley TML (1983) Clim Change 5:315

9. Carbon Dioxide Assessment Committee (1982) Changing climate. US National Research Council, National Academy, Washington, DC, USA
10. Manning WJ, Tiedemann AY (1995) Env Pollut 88:219
11. Rekas M, Szklarski Z (1990) Patent R.P. nr. 257542
12. Weppner W (1992) Mater Sci Eng B15:48
13. Yamazoe N, Miura N (1996) Solid State Ion 86–88:987
14. Kleitz M, Siebert E, Fabry P, Fouletier J (1991) Solid state potentiometric sensors. In: Göpel W, Hesse J, Zemel JN (eds) Sensors. A comprehensive survey vol 2. VCH, Weinheim, pp 341–428
15. Lee W, Nowick AS, Boaturmer LA (1986) Solid State Ion 18/19:989
16. Norby T, Kofstad P (1984) J Am Ceram Soc 67:786
17. Iwahara H, Yajima T, Hibino T, Ozaki K, Suzuki H (1993) Solid State Ion 61:65
18. Kreuer KD (1999) Solid State Ion 125:285
19. Kreuer KD (1997) Solid State Ion 97:1
20. Yajima T, Koide K, Takai H, Fukatsu N, Iwahara H (1995) Solid State Ion 79:333
21. Norby T (1990) Solid State Ion 40/41:849
22. Yaima T, Iwahara H (1992) Solid State Ion 50:281
23. Liu JF, Nowick AS (1992) Solid State Ion 50:131
24. Schreban T, Nowick AS (1989) Solid State Ion 35:189
25. Uchida H, Maeda N, Iwahara H (1983) Solid State Ion 11:117
26. Yajima T, Kaseoka H, Yogo T, Iwahara H (1991) Solid State Ion 47:271
27. Yajima T, Suzuki H, Yogo T, Iwahara H (1992) Solid State Ion 51:101
28. Iwahara H, Esaka T, Uchida H, Maeda N (1981) Solid State Ion 3\4:359
29. Iwahara H, Uchida H, Kondo J (1983) J Appl Electrochem 13:365
30. Nogata K, Nishino M, Goto KS (1987) J Electrochem Soc 134:1850
31. Iwahara H, Uchida H, Ono K, Ogaki K (1988) J Electrochem Soc 135:5239
32. Iwahara H, Uchida H, Ogaki K, Nogato H (1991) J Electrochem Soc 138:295
33. Yajima T, Koide K, Takai H, Fukatsu N, Iwahara H (1995) Solid State Ion 79:333
34. Iwahara H (1995) Solid State Ion 77:289
35. Fukatsu N, Kurita N, Koide K, Ohashi T (1998) Solid State Ion 113–115:219
36. Ma G, Shimura T, Iwahara H (1998) Solid State Ion 110:103
37. Katahira K, Matsumoto H, Iwahara H, Koide K, Iwamoto T (2000) Sens Actuators B 67:189
38. Katahira K, Matsumoto H, Iwahara H, Koide K, Iwamoto T (2001) Sens Actuators B 73:130
39. Pasierb P, Biernacka-Such A, Komornicki S, Rekas M (2006) Proc SPIE Int Soc Opt Eng 6348:634806–1
40. Lundsgaard JS, Malling J, Brichall MLS (1982) Solid State Ion 7:53
41. Murin I, Glumov OV, Samusik DB (1991) J Appl Chem USSR 64:2030
42. Pelloux A, Gondran C (1999) Sens Actuators B 59:83
43. Aono H, Yamabayashi A, Sugimoto E, Mori Y, Sadaoka Y (1997) Sens Actuators B 40:7
44. Niizeki Y, Shibata S (1998) J Electrochem Soc 145:2445
45. Matsumoto H, Kuribayashi M, Katahira K, Iwahara H (2001) Sens Actuators B 73:157
46. Gauthier M, Chamberland A (1977) J Electrochem Soc 124:1579
47. Côté R, Bale CW, Gauthier M (1984) J Electrochem Soc 131:63
48. Gauthier M, Belanger A, Fauteux D (1983) In: Chemical Sensors, Proc Intern Meeting on Chem Sensors, Fukuoka pp 353–356
49. Dubble A, Wake M, Sadaoka Y (1997) Solid State Ion 96:201
50. Dubbe A, Wiemhöfer HD, Sadaoka Y, Göpel W (1995) Sens Actuators B 24–25:600
51. Narita H, Can ZY, Mizusaki J, Tagawa H (1995) Solid State Ion 79:349
52. Zhang YC, Tagawa H, Asakura S, Mizusaki J, Narita H (1997) J Electrochem Soc 144:4345
53. Salam F, Birke P, Weppner W (1999) Electrochem Solid State Lett 2:201
54. Singh K, Ambekar P, Bhorga SS (1999) Solid State Ion 122:192
55. Jiang MRM, Weller MT, Nitrite A (1996) Sens Actuators B 30:3
56. Jacob KT, Rao DB (1979) J Electrochem Soc 126:1842
57. Gauthier M, Bellmare R, Belanger A (1981) J Electrochem Soc 128:371
58. Imanaka N, Yamaguchi Y, Adachi G, Shiokawa J (1986) J Electrochem.Soc 133:1026
59. Mari CM, Beghi M, Pizzini S, Faltemier J (1990) Sens Actuators B 2:51
60. Belanger A, Gauthier M, Fauteux D (1984) J Electrochem.Soc 131:579
61. Muruyama T, Saito Y, Matsumoto Y, Yano Y (1985) Solid State Ion 17:281
62. Rickert H (1982) Electrochemistry of solids. Springer, Berlin, p 144
63. Ogata T, Fujitsu S, Miyayama M, Koumoto K, Yamagida H (1986) J Mater Sci Letters 5:285
64. Yao S, Shimuzu Y, Miura, Yamazoe N (1990) Chem Lett:2033
65. Saito Y, Muruyama T (1988) Solid State Ion 28/30:1644
66. Miura N, Yao S, Shimizu Y, Yamazoe N (1992) J Electrochem Soc 139:1384
67. Sadaoka Y, Sakai Y, Manabe T (1993) Sens Actuators B 13–14:532
68. Liu J, Weppner W (1990) Solid State Comm 76:311
69. Liu J, Weppner W (1992) In: Balkanski M, Takahashi T, Tuller HL (eds) Solid state ionics. North-Holland, Amsterdam, pp 61–68
70. Schettler H, Liu J, Weppner W, Huggins RA (1992) Appl Phys A 57:31
71. Leonhard V, Fischer D, Erdmann H, Ilgestein M, Koppen H (1993) Sens Actuators B 13–14:530
72. Holzinger M, Maier J, Sitte W (1994) Solid State Ion 74:5
73. Holzinger M, Maier J, Sitte W (1997) Solid State Ion 94:217
74. Miura N, Yan Y, Sato M, Yao S, Shimizu Y, Yamazoe N (1994) Chem Lett:393
75. Yao S, Hosohara S, Shimizu Y, Miura N, Hutata H, Yamazoe N (1991) Chem Lett:2069
76. Shimanoe K, Kawate H, Miura N, Yamazoe N (1998) Chemical Sensors 14(Supplement A):93
77. Yao S, Shimizu Y, Miura N, Yamazoe N (1992) Jpn J Appl Phys 31:L197
78. Pasierb P, Gajerski R, Rokita M, Rekas M (2001) Physica B 304:463
79. Pasierb P, Komornicki S, Rokita M, Rekas M (2001) J Mol Structure 596:151
80. Maruyama T, Sasaki S, Saito Y (1987) Solid State Ion 23:107
81. Imanaka N, Kawasato T, Adachi G (1990) Chem Lett:497
82. Yao S, Shimizu Y, Miura N, Yamazoe N (1990) Chem Lett:2033
83. Yao S, Hosohara S, Shimizu Y, Miura N, Futata H, Yamazoe N (1990) Chem Lett:2069
84. Watabe K, Sasaki T, Ono T, Muruyama T (1991) IEEE:1002
85. Liu J, Weppner W (1991) Eur J Solid State Inorg Chem 28:1151
86. Miura N, Yao S, Shimizu Y, Yamazoe N (1991) IEEE:558
87. Sadaoka Y, Sakai Y, Manabe T (1992) J Mater Chem 2:945
88. Chu WF, Fischer D, Erdmann H, Ilgenstein M, Köppen H, Lewonhard V (1992) Solid State Ion 53–56:80
89. Miura N, Yao S, Shimizu Y, Yamazoe N (1992) J Electrochem Soc 139:1384

90. Miura N, Yao S, Shimizu Y, Yamazoe N (1992) Sens Actuators B 9:165
91. Mari CM, Narducci D, Fascheris L (1992) ISSI Lett 3:1
92. Sadaoka Y, Matsuguchi M, Sakai Y, Manabe D (1993) J Mater Sci 28:2035
93. Yao S, Shimizu Y, Miura N, Yamazoe Y (1993) Appl Phys A 57:25
94. Imanaka N, Murata T, Kawasato T, Adachi G (1993) Sens Actuators B 13–14:476
95. Miura N, Yao S, Sato M, Shimizu Y, Kuwata S, Yamazoe N (1993), Chem Lett:1973
96. Ikeda S, Kato S, Nomura K, Ito K, Einaga H, Saito S, Fujita Y (1994) Solid State Ion 70/71:569
97. Miura N, Yan Y, Sato M, Yao S, Shimizu Y, Yamazoe N (1994) Chem Lett:393
98. Lee DD, Choi SD, Lee KW (1995) Sens Actuators B 24–25:607
99. Narducci D, Facheris L, Mari CM (1995) Sens Actuators B 24–25:636
100. Imanaka N, Hirota Y, Adachi G (1995) Sens Actuators B 24–25:380
101. Ikeda S, Kondo T, Kato S, Ito K, Nomura K, Fujita Y (1995) Solid State Ion 79:354
102. Miura N, Yan Y, Nonaka S, Yamazoe N (1995) J Mater Chem 5:1391
103. Miura N, Yan Y, Sato M, Yao S, Nonaka S, Shimizu Y, Yamazoe N (1995) Sens Actuators B 24–25:260
104. Narita H, Can ZC, Mizusaki J, Tagawa H (1995) Solid State Ion 79:349
105. Holzinger M, Fleig J, Maier J, Sitte W (1995) Ber Bunsenges Phys Chem 99:1427
106. Kale GM, Davidson AJ, Fray DJ (1996) Solid State Ion 86–88:1107
107. Holzinger M, Maier J, Sitte W (1996) Solid State Ion 86–88:1055
108. Qiu F, Sun L, Li X, Hirata M, Suo H (1997) Sens Actuators B 45:233
109. Nakayama S, Kuwata S, Sato M, Sakamoto M, Sadaoka Y (1997) J Ceram Soc Jpn 105:255
110. Salam F, Bredikhin S, Birke P, Weppner W (1998) Solid State Ion 110:319
111. Aono H, Supriyatno H, Sadaoka Y (1998) J Electrochem Soc 145:2981
112. Seo MG, Kwang BH, Chai YS, Song KD, Lee DD (2000) Sens Actuators B 65:346
113. Näfe H, Aldinger F (2000) Sens Actuators B 65:46
114. Imanaka N, Kamikawa M, Tamura S, Adachi G (2000) Solid State Ion:279
115. Imanaka N, Kamikawa M, Tamura S, Adachi G (2001) Sens Actuators B 77:301
116. Alonso-Porta M, Kumar RV (2000) Sens Actuators B 71:173
117. Obata K, Kumazawa S, Shimanoe K, Miura N, Yamazoe N (2001) Sens Actuators B 76:639
118. Lee C, Akbar CA, Park CO (2001) Sens Actuators B 80:234
119. Zhang YC, Kaneko M, Uchida K, Mizusaki J (2001) J Electrochem Soc 148:H81
120. Obata K, Shimanoe K, Miura N, Yamazoe N (2003) J Mater Sci 38:4283
121. Park CO, Lee C, Akbar SA, Hwang J (2003) Sens Actuators B 88:53
122. Wang L, Kumar RV (2003) Sens Actuators B 88:292
123. Miyachi Y, Sakai G, Shimanoe K, Yamazoe N (2003) Sens Actuators B 93:259
124. Pasierb P, Komornicki S, Gajerski R, Kozinski S, Rekas M (2003) Solid State Ion 157:357
125. Pasierb P, Komornicki S, Kozinski S, Gajerski R, Rekas M (2004) Sens Actuators B 101:47
126. Menil F, Ould Daddah B, Tardy P, Debeda H, Lucat C (2005) Sens Actuators B 107:695
127. Okamoto T, Shimamoto Y, Tsumara N, Itagaki Y, Aono H, Sadaoka Y (2005) Sens Actuators B 108:346
128. Obata K, Kumazawa S, Matsushima S, Shimanoe K, Yamazoe N (2005) Sens Actuators B 108:352
129. Hong HS, Kim JW, Jung SJ, Park CO (2006) Sens Actuators B 113:71
130. Sadaoka Y (2007) Sens Actuators B 121:194
131. Aono H, Itagaki Y, Sadaoka Y (2007) Sens Actuators B 126:406
132. Satyanarayana L, Choi GP, Noh WS, Lee WY, Park JS (2007) Solid State Ion 177:3485
133. Yamauchi M, Itagaki Y, Aono H, Sadaoka Y (2008) J Europ Ceram Soc 28:27
134. Rickert, H (1982) In Electrochemistry of solids. Springer, Berlin, pp 98–101
135. Näfe H, Steinbrück M (1994) J Electrochem Soc 141:2779
136. Näfe H (1994) Sens Actuators B 21:79
137. Näfe H (1994) Solid State Ion 68:249
138. Pasierb P, Wierzbicka M, Komornicki S, Rekas M (2007) J Power Sources 173:681
139. Janata J, Josowicz M (1997) Solid State Ion 94:209
140. Fleming W (1977) J Electrochem Soc 124:21
141. Wachsman ED, Jayaweera P (2001) Solid state ionic devices II-ceramic sensors. In: Wachsman ED, Weppner W, Traversa E, Liu M, Vanysek P, Yamazoe N (eds) The potentiometric society Proc Series. Pennington, NJ, USA, pp 298–304
142. Yoo J, van Assche FM, Waschman ED (2006) J Electrochem Soc 153:H115
143. Miura N, Raisen T, Lu G, Yamazoe N (1998) Sens Actuators B 47:84
144. Garzon FH, Mukundan R, Brosha EL (2000) Solid State Ion 136–137:633
145. Miura N, Lu H, Yamazoe N (2000) Solid State Ion 136–137:533
146. Fregus JW (2007) Sens Actuators B 122:683
147. Mukundan R, Brosha EL, Brown DR, Garzon FH (2000) J Electrochem Soc 147:1583
148. Brosha EL, Mukundan R, Brown DR, Garzon FH (2002) Sens Actuators B 87:47
149. Brosha EL, Mukundan R, Brown DR, Garzon FH, Visser JH (2002) Solid State Ion 148:61
150. Guillet N, Lalauze R, Pijolat C (2004) Sens Actuators B 98:130
151. Grilli ML, Di Bartolomeo E, Lunardi A, Chevallier L, Cordiner S, Traversa E (2005) Sens Actuators B 108:319
152. Chevallier L, Di Bartolomeo E, Grilli ML, Mainas M, White B, Wachsman ED, Traversa E (2008) Sens Actuators B 129:591
153. Shimizu Y, Yamashita N (2000) Sens Actuators B 64:102
154. Ramirez-Saldago J, Fabry P (2003) Solid State Ion 158:297
155. Di Bartolomeo E, Kaabbuathong N, Grilli ML, Traversa E (2004) Solid State Ion 171:173
156. Grilli ML, Di Bartolomeo E, Lunardi A, Chevallier L, Cordiner S, Traversa E (2005) Sens Actuators B 108:319
157. Hasegawa I, Tamura S, Imanaka N (2005) Sens Actuators B 108:314
158. Xiong W, Kale GM (2006) Sens Actuators B 114:101
159. Miura N, Nakatou M, Zhuiykov S (2004) Ceram Intern 30:1135
160. Liang X, He Y, Liu F, Wang B, Zhong T, Quan B, Lu G (2007) Sens Actuators B 125:544
161. Hibino T, Hashimoto A, Kakimoto S, Sano M (2003) J Electrochem Soc 150:H279
162. Hashimoto A, Hibino T, Mori K, Sano M (2001) Sens Actuators B 81:55
163. Alberti G, Carbone A, Palombari R (2001) Sens Actuators B 75:125
164. Narayanan BK, Akbar SA, Dutta PK (2002) Sens Actuators B 87:480

165. Mukundan R, Brosha EL, Garzon FH (2003) J Electrochem Soc 150:H279
166. Zosel J, Ahlborn K, Müller R, Westphal D, Vashook V, Guth U (2004) Solid State Ion 169:115
167. Zosel J, Müller R, Vashook V, Guth U (2004) Solid State Ion 175:531
168. Dubbe A, Moos R (2006) Electrochem Solid State Lett 9:H31
169. United States Federal Register vol. 36 no. 105.
170. Graedel TE, Crutzen PJ (1993) Atmospheric change: an earth system perspective. WH Freeman, New York
171. Brüser V, Lawrenz U, Jakobs S, Möbius HH, Schönauer U (1994) Solid State Phenomena 39–40:269
172. Hötzel G, Weppner W (1986) Solid State Ion 18/19:1223
173. Hötzel G, Weppner W (1987) Sens Actuators 12:449
174. Yao S, Shimizu Y, Miura N, Yamazoe N (1991) Technical Digest of the 10th Sensor Symposium: 57
175. Shimizu Y, Okamoto Y, Yao S, Miura N, Yamazoe N (1991) Denki Kagaku 59:465
176. Yao S, Shimizu Y, Miura N, Yamazoe N (1992) Chem Lett:587
177. Yao S, Shimizu Y, Miura N, Yamazoe N (1993) Chem Lett:193
178. Miura N, Yao S, Shimizu Y, Yamazoe N (1993) Sens Actuators B 13–14:387
179. Miura N, Yao S, Shimizu Y, Yamazoe N (1994) Solid State Ion 70/71:572
180. Kurosawa H, Yan Y, Miura N, Yamazoe N (1995) Solid State Ion 79:338
181. Miura N, Iio M, Lu G, Yamazoe N (1996) Sens Actuators B 35–36:124
182. Yamazoe N, Miura N (1994) Sens Actuators B 20:95
183. Weast RC, Astle MJ (eds) (1980) CRC handbook of chemistry and physics 60th edn., CRC Press, Boca Raton, Florida pp B50–B144
184. Yao S, Shimizu Y, Miura N, Yamazoe N (1988) Denki Kagaku 61:903
185. Miura N, Lu G, Yamazoe N, Kurosawa H, Hasai M (1996) J Electrochem Soc 143:L33
186. Miura N, Kurosawa H, Hasai M, Lu G, Yamazoe N (1996) Solid State Ion 86–88:1069
187. Rao N, van der Bleek CM, Schoonman J (1992) Solid State Ion 52:339
188. Sheppard LM (1996) Ceram Industry:37
189. Jiang MRM, Weller MT (1996) Sens Actuators B 30:3
190. Shimizu Y, Maeda K (1996) Chem Letters:117
191. Akbar SA, Wanf CC, Wang L, Colling DJ (1996) Advanced Potentiometric Systems 65:331
192. Nobuhide K, Kunihiko N, and Noriyuki I (1996) Thick Film ZrO_2 NO_x Sensor. In: Proc Int Conf & Exp, Detroit, Feb. 26–29, pp 137–42
193. Zhuikov S, Miura N (2007) Sens Actuators B 121:639
194. Fergus JW (2007) Sens Actuators B 121:652
195. Gauthier M, Chamberland A, Belanger A, Poirier M (1977) J Electrochem Soc 124:1584
196. Gauthier M, Bellmare R, Belanger A (1981) J Electrochem Soc 128:371
197. Demuysere V, Bale CW (1983) Solid State Ion 9&10:1285
198. Saito Y, Muruyama T, Matsumoto Y, Kobayashi K, Yano Y (1984) Solid State Ion 14:273
199. Worell WL (1983) The application of solid -sulfate electrolytes in SO_2/SO_3 sensors. In: Chemical Sensors, Proc Intern Meeting on Chem Sensors, Fukuoka, Sep. 19–22, pp 332–337
200. Fedorov PP (1996) Solid State Ion 86–88:113
201. Mari CM, Bechi M, Pizzini S (1980) Sens Actuators B 2:51
202. Liu Q, Sun X, Wu W (1990) Solid State Ion 40/41:456
203. Liu QG, Worell WL (1986) Solid State Ion 18&19:524
204. Worell WL (1988) Solid Electrolyte Sensors for SO_2 and/or SO_3. In: Seiyama T (ed) Chemical Sensor Technology vol.1, pp 97–108
205. Kriedl EL, Simon I (1958) Nature 181:1529
206. El-Kabbany FAI (1980) Phys Stat Sol (a) 58:373
207. Kvist A, Lundén A (1965) Z Naturforschg 20:235
208. Imanaka N, Yamaguchi Y, Adachi G, Shiokawa J (1985) J Electrochem Soc 132:2519
209. Imanaka N, Yamaguchi Y, Adachi G, Shiokawa J, Yoshioka H (1986) Solid State Ion 20:153
210. Imanaka N, Adachi G, Shiokawa J (1983) Na_2SO_4 doped with $NaVO_3$ and/or $Ln_2(SO_4)_3$ (Ln= Rare Earths) as an SO_2 solid electrolyte sensor. In: Proc Int Meeting on Chemical Sensor Fukuoka, Sep. 19–22 pp 348–52
211. Rog G, Kozlowska-Rog A, Zakula K (1991) J Appl Electrochem 21:308
212. Jang PH, Jang JH, Chen CS, Peng DK, Meng GY (1996) Solid State Ion 86–88:1095
213. Itoh M, Kozuka Z (1986) J Electrochem Soc 133:1512
214. Jinhua Y, Pinghua Y, Guangyao M (1996) Sens Actuators B 31:209
215. Rao N, Becht JGM, Sørensen OT, Schoonman J (1991) ISSI Lett 2:13
216. Saito Y, Muruyama T, Matsumoto Y, Yano Y (1983) Electromotive force of the SO_2–O_2–SO_3 concentration cell using NASICON ($Na_3Zr_2Si_2PO_{12}$) as a solid electrolyte. In: Chemical Sensors, Proc Intern Meeting on Chem Sensors, Fukuoka, pp 326–331
217. Muruyama T, Saito Y, Matsumoto Y, Yano Y (1985) Solid State Ion 17:281
218. Choi SD, Chung WY, Lee DD (1996) Sens Actuators B 35–36:263
219. Meng GY, Rao NL, Jensen PV, Sørensen OT (1990) Evaluation of the potentiometric SO_x (x=2, 3) sensor with a tubular NASICON electrolyte. In: Chowdari BVR, Liu QG, Chen LQ (eds) Recent advances in fast ion conducting materials and devices, World Sci Publ Comp, pp 375–379
220. Rao N, van den Bleek CM, Schoonman J, Sørensen OT (1992) Solid State Ion 53–56:30
221. Akila R, Jacob KT (1988) J Appl Electrochem 18:245
222. Akila R, Jacob KT (1989) Sens Actuators B 16:311
223. Yan Y, Shimizu Y, Miura N, Yamazoe N (1994) Sens Actuators B 20:81
224. Zhuiykov S (1999) Fuel 79:1255
225. Yan Y, Shimizu Y, Miura N, Yamazoe N (1993) Sens Actuators B 12:77
226. Yan Y, Miura N, Yamazoe N (1996) J Electrochem Soc 143:609
227. Skeaff JM, Dubreuil AA (1993) Sens Actuators B 10:161
228. Azad AM, Akbar SA, Mhaisalkar SG, Birkefeld LD, Goto KS (1992) J Electrochem Soc 139:3690
229. Kitzelman D, Deprez J (1980) German Patent Application DE 3033 796 A I
230. Yasuda A, Yamaga N, Doi K, Fuijoka T, Kusanagi S (1992) J Electrochem Soc 139:1091
231. Tan Y, Tan TC (1995) Sens Actuators B 28:113
232. Li N, Taa TC, Zeng HC (1993) J Electrochem Soc 140:1068
233. Lucas Z, Sinz M, Staikov G, Lorenz WJ, Baier G, Vogel A (1994) Solid State Ion 68:93
234. Can ZY, Narita H, Mizusaki J, Tagawa H (1995) Solid State Ion 79:344
235. Miura N, Raisen T, Lu G, Yamazoe N (1997) J Electrochem Soc 144:L198
236. Miura N, Raisen T, Lu G, Yamazoe N (1998) Sens Actuators B 47:84
237. Sorita R, Kawano T (1996) Sens Actuators B 35–36:274
238. Sorita R, Kawano T (1997) Sens Actuators B 40:29
239. Fergus JW (2007) Sens Actuators B 122:683
240. Hibino T, Kuwahara Y, Kuroki Y, Oshima T, Inoue R, Kitanoya S, Fuma T (1997) Solid State Ion 104:163